Table 3
EDX analysis on doubly sintered PMN ceramics derived from a corundum *B*-site precursor route.

Dielectric properties (1 kHz)	Sintering temperatures (T_1/T_2) (°C) and dwell time of each step (h)				
	Columbite-route		Corundum-route		
	1275, 2 (Ref. [20])	1025/1100, 2 (Ref. [14])	1025/1000, 1	1050/1025, 1 (this work)	1075/1025, 1
$\varepsilon_{r,25\,^\circ C}$	18,268	9,500	15,372	18,313	19,023
Tan $\delta_{25\,^\circ C}$	0.01	0.001	0.001	0.004	0.009
$T_{\varepsilon_{r,max}}$	−9	−10	−17.5	−16.3	−15
$\varepsilon_{r,max}$	24,003	13,910	20,708	23,823	24,291
tan δ_{max}	0.20	0.12	0.11	0.12	0.14
Diffusivity (γ)	–	–	1.79	1.66	1.67

indication of close to completely disordered relaxor behavior in the ceramics sintered by this route.

Here, the effect of two-stage sintering on phase formation, microstructure and dielectric properties of the PMN ceramics derived from a corundum *B*-site precursor route was investigated and compared with both the normal and the two-stage sintered columbite-routes. The different microstructural characteristics, density and amount of secondary phase present in sintered PMN ceramics strongly influence the dielectric properties of these materials, leading to superior electrical behavior in two-stage sintered corundum-route PMN sample. In comparison to the normal sintering method, although a disadvantage of the proposed two-stage sintering method is a greater time requirement, the significant reduction in firing temperature is a possible development, particularly with regard to the drive towards electrodes of lower cost for electronic products [1,2,26]. In general, these PMN ceramics exhibit complex microstructures which are a result of variation in grain size, shape and orientation, variation in chemical homogeneity and densification, and the presence of additional minor phase, pores and (micro) cracks. These factors, which are strongly influence by the sintering conditions, have an important effect on the dielectric properties. Furthermore, the PMN ceramics showed a comparable perovskite yield, maximum density, and dielectric properties to those obtained by the partial oxalate [36], or even better than those fabricated by the sol–gel [11], the freeze-drying [41], and the citrate-gel [42] methods.

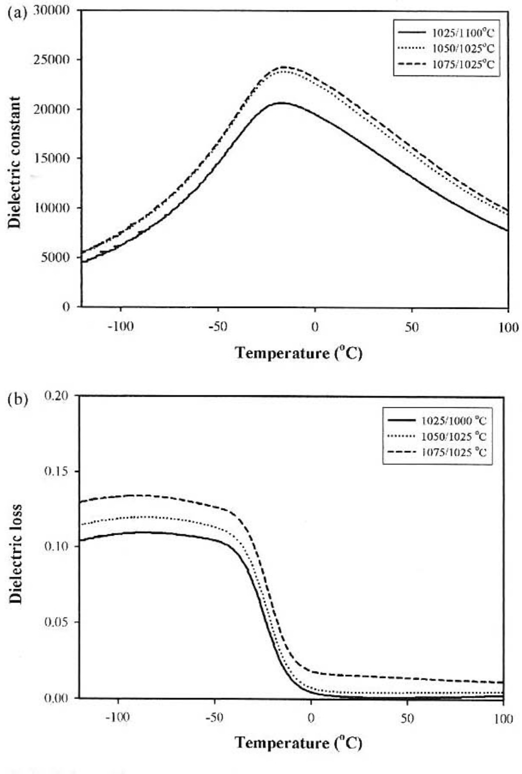

Fig. 4. Variation with temperature of: (a) dielectric constant and (b) dielectric loss at 1 kHz for PMN ceramics doubly sintered at various conditions.

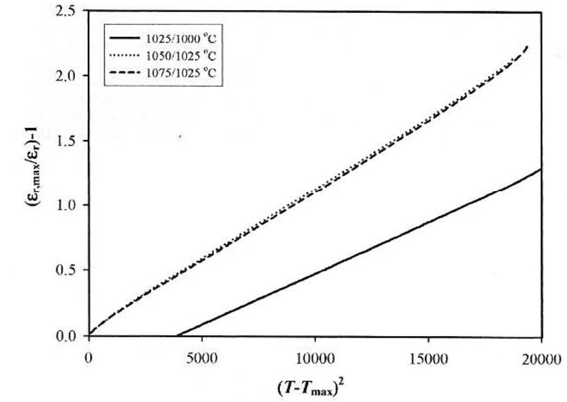

Fig. 5. Dependence of $(\varepsilon_{r,max}/\varepsilon_r)-1$ with $(T-T_{max})^2$ for PMN ceramics doubly sintered at various conditions.

4. Conclusion

This work demonstrated that, under suitable processing conditions, the properties of the PMN ceramics derived from a combination between the corundum *B*-site precursor and the two-stage sintering methods are equivalent to (or even better than) those obtained from a well-known columbite route (either a normal or a two-stage sinterings). It has been found that the two-stage sintering can effectively suppress the grain growth in perovskite PMN.

Acknowledgements

This work was supported by the Thailand Research Fund (TRF) and the Commission on Higher Education (CHE).

References

[1] A.J. Moulson, J.M. Herbert, Electroceramics, 2nd ed., Wiley, Chichester, 2003.
[2] G.H. Haertling, J. Am. Ceram. Soc. 82 (1999) 797.
[3] I.V. Kityk, M. Makowska-Janusik, M.D. Fontana, M. Aillerie, A. Fahmi, Cryst. Res. Technol. 36 (2001) 577.
[4] S.J. Jang, L.E. Cross, K. Uchino, J. Am. Ceram. Soc. 64 (1981) 209.

[5] M. Lejeune, J.P. Boilot, Ceram. Int. 8 (1982) 99.
[6] S.L. Swartz, T.R. Shrout, W.A. Schulze, L.E. Cross, J. Am. Ceram. Soc. 67 (1984) 311.
[7] J. Chen, A. Gorton, H.M. Chen, M. Harmer, J. Am. Ceram. Soc. 69 (1986) C303.
[8] S.L. Swartz, T.R. Shrout, Mater. Res. Bull. 17 (1982) 1245.
[9] M. Lejeune, J.P. Boilot, Am. Ceram. Soc. Bull. 64 (1984) 679.
[10] J.P. Guha, H.U. Anderson, J. Am. Ceram. Soc. 69 (1986) C287.
[11] F. Chaput, J.P. Boilot, M. Lejeune, R. Papiernik, L.G. Pfaizgrag, J. Am. Ceram. Soc. 72 (1989) 1355.
[12] Y.C. Liou, J.H. Chen, Ceram. Int. 30 (2004) 17.
[13] K. Sreedhar, A. Mitra, Mater. Res. Bull. 32 (1997) 1643.
[14] P.A. Joy, K. Sreedhar, J. Am. Ceram. Soc. 80 (1997) 770.
[15] S. Ananta, N.W. Thomas, J. Eur. Ceram. Soc. 19 (1999 2917).
[16] R. Wongmaneerung, T. Sarakonsri, R. Yimnirun, S. Ananta, Mater. Sci. Eng. B 132 (2006) 292.
[17] R. Wongmaneerung, T. Sarakonsri, R. Yimnirun, S. Ananta, Mater. Sci. Eng. B 130 (2006) 246.
[18] S. Ananta, Mater. Lett. 58 (2004) 2530.
[19] S. Ananta, Mater. Lett. 58 (2004) 2834.
[20] R.L. Fullman, Trans. AIME 197 (1953) 447.
[21] S. Ananta, N.W. Thomas, J. Eur. Ceram. Soc. 19 (1999) 629.
[22] S. Ananta, N.W. Thomas, J. Eur. Ceram. Soc. 19 (1999) 155.
[23] Powder Diffraction File No. 81-861, International Centre for Diffraction Data, Newton Square, PA, 2000.
[24] H.C. Ling, A.M. Jackson, M.F. Yan, W.W. Rhodes, J. Mater. Res. 5 (1990) 629.
[25] Powder Diffraction File No. 82-338, International Centre for Diffraction Data, Newton Square, PA, 2000.
[26] P. Lucas, W.T. Petuskey, J. Am. Ceram. Soc. 84 (2001) 2150.
[27] H.T. Kim, Y.H. Han, Ceram. Int. 30 (2004) 1719.
[28] S.H. Hur, J.K. Lee, K.W. Park, H.S. Hong, S.J. Park, Mater. Lett. 35 (1998) 78.
[29] W. Chaisan, R. Yimnirun, S. Ananta, Ferroelectrics 346 (2007) 84.
[30] M.H. Lin, J.F. Chou, H.Y. Lu, J. Eur. Ceram. Soc. 20 (2000) 517.
[31] O. Guillon, F. Thiebaud, D. Perreux, C. Courtoris, P. Champagne, A. Leriche, J. Crampon, J. Eur. Ceram. Soc. 25 (2005) 2421.
[32] C.E. Seo, D.Y. Yoon, J. Am. Ceram. Soc. 88 (2005) 963.
[33] U.J. Chung, J.k. Park, N.M. Hwang, H.Y. Lee, D.Y. Kim, J. Am. Ceram. Soc. 85 (2002) 965.
[34] S.B. Lee, N.M. Hwang, D.Y. Yoon, M.F. Henry, Metal. Mater. Trans. A 31 (2000) 985.
[35] H.K. Lee, J.S. Kim, N.M. Hwang, D.Y. Kim, J. Eur. Ceram. Soc. 20 (2000) 731.
[36] S.M. Gupta, C.S. Harendranath, A.R. Kulkarni, Ceram. Int. 23 (1997) 191.
[37] R. Wongmaneerung, R. Yimnirun, S. Ananta, Appl. Phys. A 86 (2007) 249.
[38] C.H. Lu, J.T. Lee, J. Ceram. Soc. Jpn. 103 (1995) 1122.
[39] R. Rai, S. Sharma, Solid State Commun. 129 (2004) 305.
[40] E.F. Alberta, A.S. Bhalla, J. Phys. Chem. Sol. 63 (2002) 1759.
[41] W.B. Ng, J. Wang, S.C. Ng, L.M. Gan, J. Mater. Chem. 8 (1998) 2239.
[42] Y.S. Hang, H.B. Park, S.J. Kim, J. Eur. Ceram. Soc. 18 (1998) 613.

Ferroelectrics, 403:150–157, 2010
Copyright © Taylor & Francis Group, LLC
ISSN: 0015-0193 print / 1563-5112 online
DOI: 10.1080/00150191003750853

Taylor & Francis
Taylor & Francis Group

Effects of ZnO Nanowhiskers Addition on Microstructure and Dielectric Properties of Lead Titanate Ceramics

R. WONGMANEERUNG,[1],* S. CHOOPAN,[2] R. YIMNIRUN,[3]
AND S. ANANTA[2]

[1]Department of Physics, Faculty of Science, Maejo University,
Chiang Mai 50290, Thailand
[2]Department of Physics and Materials Science, Faculty of Science,
Chiang Mai University, Chiang Mai 50200, Thailand
[3]School of Physics, Institute of Science, Suranaree University of Technology,
Nakhon Ratchasima 30000, Thailand

Ceramic nanocomposites of zinc oxide (ZnO) nanowhiskers in lead titanate ($PbTiO_3$ or PT) matrix were successfully fabricated by a pressureless sintering technique. Phase formation, densification, microstructure and dielectric properties of the composites were investigated as a function of ZnO content. It has been found that a densification of the ceramic nanocomposites fabricated in this work was significantly enhanced, as compared to the conventional PT ceramics. Moreover, the high dielectric constant, which is higher than that of the monolithic PT ceramics, was found in the PT/ZnO ceramic nanocomposites.

Keywords Lead titanate; perovskite; nanocomposites; dielectric properties

1. Introduction

Recently, ceramic nanocomposites in which nanosized phases were dispersed within the matrix grains and/or at the grain boundaries have emerged as a novel approach of improving material properties [1–6]. In order to improve the dielectric properties of ferroelectric ceramics, nanocomposites consisting of two or more materials with different macroscopic properties are more attractive than their single-phase counterparts due to the improvement in both the physical and mechanical properties. However, most nanocomposites studied are derived from a combination of piezoelectric ceramics and polymers [7, 8]. Few studies have reported on ferroelectric matrix/metal nanodispersoid [9] and non-ferroelectric matrix/ferroelectric nanodispersoid [6] composite systems. Little work has been undergone on the preparation of piezoelectricity/semiconductor PZT/ZnO composites [10, 11] with high dielectric permittivity. It has been found that the presence of large amounts of semiconductor nanosized ZnO particles in the PZT matrix ceramics can result in a significantly increase of dielectric properties. Interestingly, no work on PT/ZnO composites (or nanocomposites)

Received August 23, 2009; in final form September 30, 2009.

*Corresponding author. E-mail: re_nok@yahoo.com ever been reported so far. Thus, in this work, small amount ZnO nanowhiskers (0.1–1.0 wt%) reinforced PT ceramics are fabricated by conventional sintering technique. The effects of ZnO nanowhiskers addition on microstructure and dielectric properties of the composites have been discussed.

2. Experimental

The PT/ZnO ceramic nanocomposites were prepared by using the conventional solid-state reaction and subsequent pressureless sintering process. The starting materials were PT powders (average particle size ∼0.3–2 μm) and ZnO nanowhiskers (average diameter ∼0.4–2 μm and ∼12–36 μm in length), as shown in Fig. 1. Characteristic properties of starting materials and detail of these fabrication procedures were already described elsewhere [12, 13]. Briefly, different amounts (0.1–1.0 wt%) of ZnO nanowhiskers were ultrasonically dispersed in ethanol for 10 min before vibro-mixing with the PT powders. The powder mixtures were form into pellet by adding 3 wt% polyvinyl alcohol (PVA) binder, prior to pressing in a uniaxial press at 100 MPa. Each pellet was placed in a closed

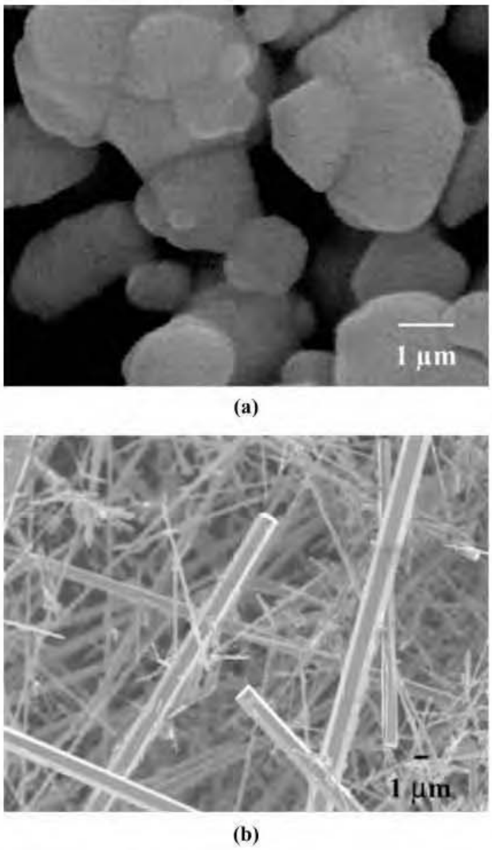

Figure 1. SEM micrographs of the starting materials: (a) PT powders and (b) ZnO nanowhiskers.

alumina crucible with an atmosphere powder of identical chemical composition [14]. The PVA binder was burnt out at 550°C with heating rate of 10°C/min and sintered at 1200°C for 2 h with heating/cooling rates of 1°C/min order to avoid the sample damage after sintering [14, 15].

Densities of the samples were determined by the Archimedes method. Phase analysis was performed on X-ray diffraction (XRD) (Siemens-D500). The tetragonality factor of the samples was calculated from the XRD patterns [15]. The microstructural development was characterized using a scanning electron microscopy (SEM) (JEOL JSM-840A). The grain sizes of the samples were measured by employing the linear intercept method [14, 15]. The dielectric measurement of the flat polished samples was performed with the LCR meter (HIOKI 3532-50) at 1 MHz and temperature range from 150 to 550°C as a decrease in temperature. The samples were coated with silver paste electrode which was fired on both sides of the samples at 550°C for 1 h.

3. Results and Discussion

As shown in Fig. 2, in general, no measurable change in *d*-spacing for samples containing different ZnO content was observed. All the XRD peaks were identified as tetragonal $PbTiO_3$, which could be matched with JCPDS file no. 6-452 [16], in agreement with other works [3–6]. The diffraction peaks of ZnO in the nanocomposites were not intense possibly because its amount was less than the XRD detection limits (~5 wt% [12, 15]). As listed in Table 1, the density values increased slightly with increasing the content of ZnO nanowhiskers and the values of all nanocomposite samples are higher than those observed in monolithic PT ceramics. It indicates the effect of ZnO nanowhiskers addition on the sinterability of PT ceramics. By comparison with conventional monolithic PT ceramics, lower values of tetragonality factor are found in all composite cases, indicating lower internal stress in these nanocomposites consistent with other similar systems [5, 6]. One explanation for the decrease in tetragonality of the PT/ZnO could be the incorporation

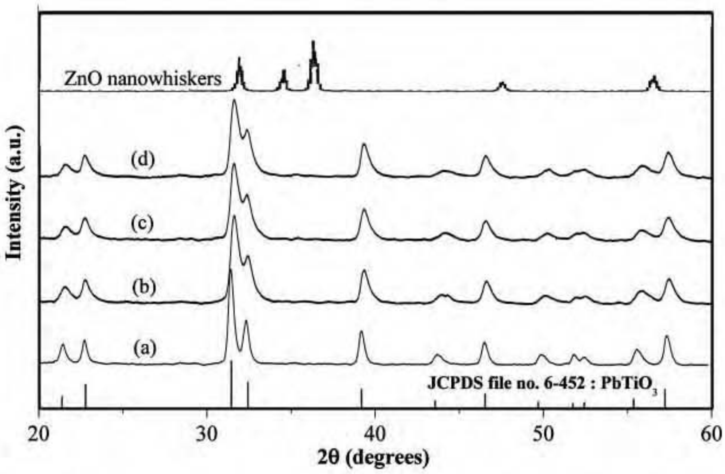

Figure 2. XRD patterns of PT ceramic-nanocomposites reinforced with ZnO nanowhiskers: (a) 0.0, (b) 0.1, (c) 0.5 and (d) 1 wt%.

Table 1

Physical and dielectric properties of PT/ZnO ceramic-nanocomposites

	Physical Properties				Dielectric Properties at 1 MHz		
Processing [Ref.]	Additive (wt%)	Tetragonality (c/a)	Relative density (%)	Grain size[a] (mean) (μm)	T_C (°C)	$\varepsilon_{r,max}$	$\tan\delta_{max}$
Composite reinforced with ZnO nanowhiskers	0.0	1.063	94	0.6–2.0 (1.4)	482	7680	1.07
	0.1	1.061	96	0.5–1.7 (0.8)	468	11406	0.80
	0.5	1.061	98	0.3–1.3 (0.7)	465	11050	1.40
	1.0	1.060	98	0.3–1.0 (0.7)	478	9696	1.18
Composite reinforced with SiC nanofibers [10]	0.1	1.061	95	0.5–2.2 (0.8)	485	9337	0.76
	0.5	1.061	91	0.5–2.6 (0.7)	—	—	—
	1.0	1.060	90	0.2–1.6 (0.6)	482	5493	1.18

[a] The estimated precision of the grain size is ± 10%.

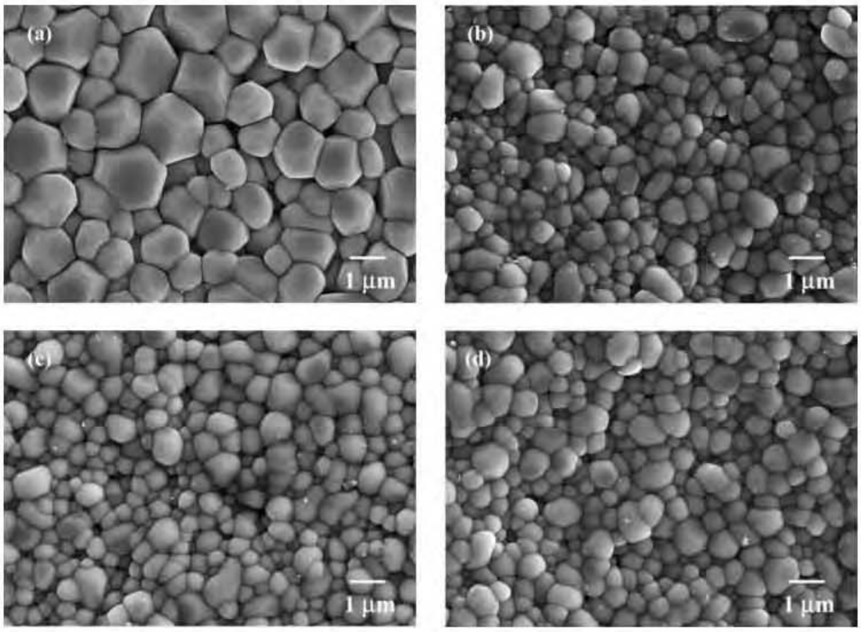

Figure 3. SEM micrographs of PT ceramic-nanocomposites reinforced with ZnO nanowhiskers: (a) 0.0, (b) 0.1, (c) 0.5 and (d) 1 wt%.

of Zn ions into the PT lattice during sintering, as the case in the other systems [17]. More interestingly, all samples have not been broken into small pieces after experienced the sintering process or once subjected to a cycle of high temperature measurement of dielectric properties.

Microstructural examination of the monolithic PT ceramics and PT/ZnO composites sintered at 1200°C for 2 h are displayed in Fig. 3. The grain structure of monolithic PT ceramics showed spherical shape and poor packing. On the other hand, microstructures of PT/ZnO nanocomposites were uniform equiaxed with good grain-packing as shown in Fig. 3 (b)–(d). These microstructures are typical of a solid-state sintering mechanism with the "intergranular" structural model of ceramic nanocomposites proposed by Niihara *et al.* [1]. The average grain sizes were found to decrease significantly with the content of ZnO. It seems that the ZnO nanowhiskers dispersed in the PT matrix control grain boundary movement and limit the grain growth of the PT matrix as earlier observed in other similar systems [3, 4]. In comparison with the typical monolithic PT [14, 15], almost clean microstructure with highly uniform, dense, angular grain-packing and more homogenous are observed. Furthermore, it should be noted that the average grain size of all PT/ZnO nanocomposites is less than the critical value of 3 μm [14] and gives rise to a volumetric percentage enough to buffer the anisotropic stress caused by the phase transition [15]. The reduced grain size of the composites is considered to be responsible for the improvement of their mechanical properties [18].

Figure 4 shows the variations of dielectric constant and dielectric loss at 1 MHz with ZnO contents at various temperatures. The ferroelectric-paraelectric phase transition

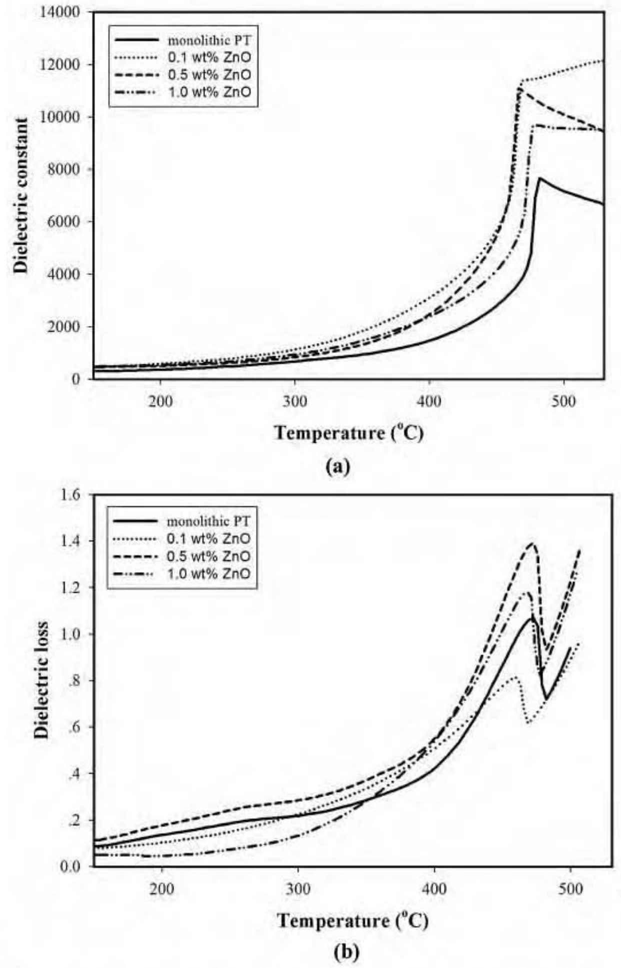

Figure 4. Variation with temperature of (a) dielectric constant and (b) dielectric loss at 1 MHz of PT ceramic-nanocomposites reinforced with ZnO nanowhiskers at various contents.

temperature (T_C) is also listed in Table 1. Generally, they all behave as typical normal ferroelectric materials [3, 4]. Similar trend in dielectric values at T_C was also observed. It is evident that the addition of 0.1%wt ZnO to PT leads to drastic increase in the dielectric constant maximum. The dielectric constant of the composites then decreases with further ZnO additions up to 1.0%wt but still higher than those of the monolithic PT ceramics which could be attributed to the effects of ZnO content, as earlier proposed in the PZT/ZnO systems [10, 11], in associated with a decrease in porosity. It can be said that the ZnO phase showed a chemical reaction with ferroelectric phase when the composites were sintered at high temperature. Another possible reason is that the presence of large amounts of semiconductor ZnO nanowhisker in the ferroelectric PT matrix ceramics can result in a significant increase of dielectric properties. By comparison with our earlier work on the PT/SiC nanocomposites system [6], the dielectric properties were decreased with increasing the amount of SiC which is non-ferroelectric phase. On the other hand, semiconducting ZnO in electric materials could improve electrical properties. Moreover, it is seen that with the increase of ZnO content, the peak of T_C shifted towards lower temperatures (Table 1 and Fig. 4) which could be due to a relaxation of transformation-induced internal stress by the ZnO whiskers randomly dispersed in the PT matrix [10].

The results obtained in this work suggest that these PT/ZnO composites exhibit complex microstructures which are inherently heterogeneous. The heterogeneity is a result of variation in grain size, whiskers length and orientation, variation in chemical homogeneity; and the presence and distribution of additional phase and pores. These factors have an important effect on the dielectric properties of the materials.

4. Conclusions

Perovskite ferroelectric lead titanate ceramic-nanocomposites embedded with semiconductor ZnO nanowhiskers can be successfully fabricated by using a simple, inexpensive solid-state reaction under pressureless sintering method. Compared with the conventional monolithic PT ceramics, addition of ZnO nanowhiskers was found to enhance densification, mechanical and dielectric properties of PT-based ceramics significantly.

Acknowledgment

This work was supported by the Thailand Research Fund (TRF), the Commission on Higher Education (CHE), the National Nanotechnology Center (NANOTEC) and the Faculty of Science, Chiang Mai University and Maejo University.

References

1. K. Niihara, A. Nakahira, and T. Sekino, Nanophase and nanocomposite materials. *J. Ceram. Soc. Jpn.* **99**, 405–412 (1991).
2. J. D. Kuntz, G. D. Zhan, and A. K. Mukherjee, Nanocrystalline-matrix ceramic composites for improved fracture toughness. *MRS Bull.* **29**, 22–27 (2004).
3. R. Wongmaneerung, R. Yimnirun, and S. Ananta, Fabrication and characterization of perovskite ferroelectric PMN/PT ceramic nanocomposites. *J. Mater. Sci.* **44**, 5428–5440 (2009).
4. R. Wongmaneerung, R. Yimnirun, and S. Ananta, Potential of nanocomposite technique for fabrication of smart ceramics. *Chiang Mai J. Sci.* **36**, 179–187 (2009).
5. R. Wongmaneerung, A. Rujiwatra, R. Yimnirun, and S. Ananta, Fabrication and dielectric properties of lead titanate nanocomposites. *J. Alloy. Compd.* **475**, 473–478 (2009).
6. R. Wongmaneerung, P. Singgai, R. Yimnirun, and S. Ananta, Effects of SiC nanofibers addition on microstructure and dielectric properties of lead titanate ceramics. *J. Alloy. Compd.* **475**, 456–462 (2009).
7. V. Srikant and D. R. Clarke, On the optical band gap of zinc oxide. *J. Appl. Phys.* **83**, 5447 (1998).
8. R. E. Newnham, Smart, very smart, and intelligent materials. *MRS Bull.* **22**, 20 (1997).
9. H. J. Hwang, K. Watari, M. Sando, M. Toriyama, and K. Niihara, Low-temperature sintering and high-strength Pb(Zr,Ti)O_3-matrix composites incorporating silver particles. *J. Am. Ceram. Soc.* **80**, 791–793 (1997).
10. Z. M. Dang, D. Xie, S. G. Lu, and S. C. Tjong, Morphology and dielectric properties of lead zirconate titanate/nano-ZnO composites. *Key. Eng. Mater.* **280–283**, 171–174 (2005).

11. M. S. Cao, W. Zhou, X. L. Shi, and Y. J. Chen, Dynamic response and reinforcement mechanism of composites embedded with tetraneedlelike ZnO nanowhiskers. *Appl. Phys. Lett.* **91**, 021912 (2007).
12. R. Wongmaneerung, R. Yimnirun, and S. Ananta, Effect of vibro-milling time on phase formation and particle size of lead titanate nanopowders. *Mater. Lett.* **60**, 1477–1452 (2006).
13. S. Choopan, N. Hongsith, S. Tanunchai, T. Chairuangsai, P. Mangkorntong, and N. Mangkorntong, Single-crystalline ZnO nanobelts by RF sputtering. *J. Cryst. Growth.* **282**, 365–369 (2005).
14. A. Udomporn, K. Pengpat, and S. Ananta, Highly dense lead titanate ceramics from refined processing. *J. Eur. Ceram. Soc.* **24**, 185–188 (2005).
15. R. Wongmaneerung, R. Yimnirun, and S. Ananta, Effects of sintering condition on phase formation, microstructure and dielectric properties of lead titanate ceramics. *Appl. Phys. A.* **86**, 249–255 (2007).
16. JCPDS-ICDD Card no. 6-452. *International Centre for Diffraction Data*. Newtown Square. PA, 2000.
17. P. H. Xiang, X. L. Dong, C. D. Feng, N. Zhong, and J. K. Guo, Sintering behavior, mechanical and electrical properties of lead zirconate Titanate/NiO composites from coated powders. *Ceram. Int.* **30**, 765–772 (2004).
18. T. Suwannasiri and A. Safari, Effect of rare-earth additives on electromechanical properties of modified lead titanate ceramics. *J. Am. Ceram. Soc.* **76**, 3155–3158 (1993).

Journal of Alloys and Compounds 509 (2011) 3547–3552

Contents lists available at ScienceDirect

Journal of Alloys and Compounds

journal homepage: www.elsevier.com/locate/jallcom

Dielectric properties of $PbTiO_3$/ZnO ceramic nanocomposites obtained by solid-state reaction method

R. Wongmaneerung[a,*], S. Choopan[b], R. Yimnirun[c], S. Ananta[b]

[a] Materials Science Program, Faculty of Science, Maejo University, Chiang Mai 50290, Thailand
[b] Department of Physics and Materials Science, Faculty of Science, Chiang Mai University, Chiang Mai 50200, Thailand
[c] School of Physics, Institute of Science, Suranaree University of Technology, Nakhon Ratchasima 30000, Thailand

ARTICLE INFO

Article history:
Received 30 July 2010
Received in revised form 3 December 2010
Accepted 3 December 2010
Available online 10 December 2010

Keywords:
Ferroelectric
Lead titanate
Zinc oxide
Dielectric response
Nanocomposites

ABSTRACT

In this paper, we report on the dielectric properties of $PbTiO_3$/ZnO ceramic nanocomposites prepared by a conventional solid-state reaction method with improvement in densification by the addition of ZnO nanowhiskers. Phase formation, densification, microstructure and dielectric properties of the composites were investigated as a function of the content of ZnO nanowhiskers. Densification behavior of the ceramic nanocomposites was significantly enhanced, as compared to pure $PbTiO_3$ ceramics. Moreover, the dielectric constant of the composites was higher than that of the pure $PbTiO_3$ ceramics.

1. Introduction

Dense perovskite lead titanate ($PbTiO_3$ or PT) based ceramics are known to exhibit excellent dielectric, piezoelectric and pyroelectric properties for use in electronic and electro-optic devices at high temperatures and high frequencies [1]. However, it is well known that pure PT ceramics are difficult to obtain because they break up into powders when they are cooled down through the Curie point, due to the large distortion of the tetragonal phase at room temperature (which is characterized by a c/a ratio of ~1.06) [2,3]. Therefore, dielectric properties of PT ceramics are only available for porous and doped samples. Also, such samples usually have very high conductivity at elevated temperatures.

The concept of a functionally graded material has been used to overcome the mechanical problems. Piezoelectric ceramic/ceramic functionally graded materials have been studied in order to reduce the stress concentration in the actuators [4,5]. However, problems still exist with the thermal expansion mismatch. Several approaches to improve the mechanical strength of the composites by incorporating polymers, metals, fibers or whiskers have been investigated [6–10].

In an attempt to improve the dielectric properties of ferroelectric ceramics, ceramic nanocomposites consisting of two or more components with different macroscopic properties have shown promise due to the improvement in both physical and mechanical properties. In the past few years, additional attempts have been carried out by the addition of oxide particles such as ZrO_2 and MgO [11–13]. Moreover, piezoelectric nanocomposites embedded with ZnO whiskers, such as PZT/ZnO composites, have been prepared through a normal sintering process in air. The composites not only retained good piezoelectric properties, but also exhibited excellent and significantly improved mechanical properties. A few studies have been conducted on ferroelectric matrix/metal nanodispersoid [14] and non-ferroelectric matrix/ferroelectric nanodispersoid [15]. PT ceramic-based composites have recently been developed to improve the mechanical and dielectric properties [16,17]. Silicon carbide (SiC) nanofibers and PT nanopowders have been employed as the reinforcement in the composites because of their ability to resist crack growth [18]. However, the addition of SiC nanofibers leads to reduced dielectric constant. ZnO has received much attention as a reinforced composite material due to its high-temperature strength and excellent chemical stability [19]. No work on PT/ZnO composites has yet been reported. In this paper, PT ceramics doped with ZnO nanowhiskers (0.1–5.0 wt%) were fabricated by a conventional solid-state reaction method. Effects of the ZnO nanowhiskers on the microstructure and dielectric properties of the composites were studied and discussed.

---

[*] Corresponding author. Tel.: +66 53 873515.
E-mail address: re_nok@yahoo.com (R. Wongmaneerung).

0925-8388/$ – see front matter © 2010 Elsevier B.V. All rights reserved.
doi:10.1016/j.jallcom.2010.12.024

Table 1
Physical properties of PT/ZnO composites sintered at 1200 °C for 2 h.

ZnO nanowhisker (wt%)	Perovskite phase[a] (%)	Tetragonality (*c*/*a*)	Relative density (%)	Grain size[b] (mean) (µm)
0.0	100.00	1.063	94	20.0–65.0 (36)
0.1	100.00	1.061	96	0.5–1.7 (0.8)
0.5	100.00	1.061	98	0.3–1.3 (0.7)
1.0	100.00	1.060	98	0.3–1.0 (0.7)
3.0	98.56	1.061	97	0.5–2.2 (1.6)
5.0	95.23	1.060	98	0.7–3.7 (2.0)

[a] The estimated precision of the perovskite phase is ±0.1%.
[b] The estimated precision of the grain size is ±10%.

2. Experimental

PT/ZnO ceramic nanocomposites were prepared using the conventional solid-state reaction and subsequent pressureless sintering process. Commercially available powders of PbO (Fluka, >99.9% purity) and TiO_2 (Aldrich, >99.9% purity) were used as raw materials to produce PT powders. Composites were made with the synthesized PT powders (average particle size ~1–5 µm) and ZnO nanowhiskers [20] (average diameter ~0.4–2 µm and ~12–36 µm length), as shown in Fig. 1. Different amounts (0.1–5.0 wt%) of ZnO nanowhiskers were ultrasonically dispersed in ethanol for 10 min before vibro-mixing with the PT powders. The powder mixtures were formed into pellets by adding 3 wt% polyvinyl alcohol (PVA) binder, prior to pressing in a uniaxial press at 100 MPa. For sintering, the pellets were placed in a closed alumina crucible with an atmosphere powder of identical chemical composition [16,17]. The PVA binder was burnt out at 550 °C. Samples were sintered at 1200 °C for 2 h at heating/cooling rates of 5 °C/min.

Densities of the sintered samples were measured by the Archimedes method. Phase analysis was performed by X-ray diffraction (XRD) (Siemens-D500). Tetragonality factors of the ceramic nanocomposites were calculated from the XRD patterns [21]. Microstructures of the samples were characterized using a scanning electron microscope (SEM) (JEOL JSM-840A). Grain sizes of the sintered ceramics were measured by employing the linear intercept method. In order to evaluate dielectric properties, dense ceramic nanocomposites were polished to form flat and parallel faces. The samples were coated with silver paste electrode which was fired on both sides of the samples at 550 °C for 1 h. Dielectric measurement of the sintered ceramics was performed with an LCR meter (HIOKI 3532-50). All measurements were conducted over a frequency range from 1 to 5 MHz and a temperature range from 550 °C to 25 °C.

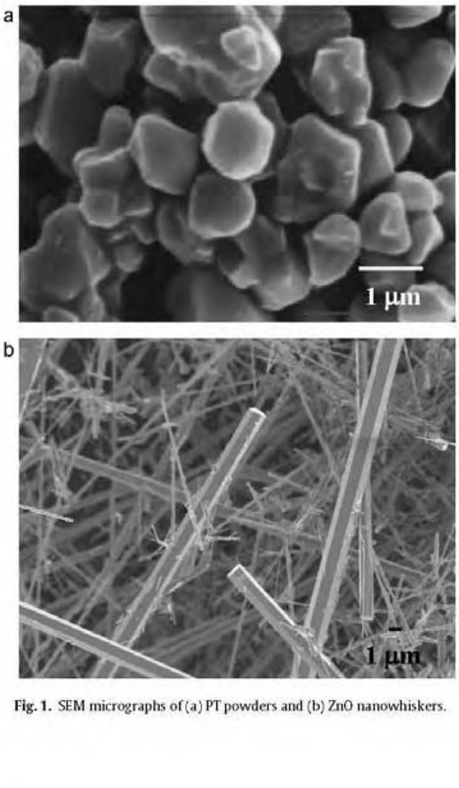

Fig. 1. SEM micrographs of (a) PT powders and (b) ZnO nanowhiskers.

Table 2
Dielectric properties of PT/ZnO composites measured at 1 MHz.

ZnO nanowhisker (wt%)	T_C (°C)	$\varepsilon_{25\,°C}$	$\tan\delta_{25\,°C}$	$\varepsilon_{r,max}$	$\tan\delta_{max}$
0.0	482	243	0.02	7680	1.07
0.1	468	350	0.06	11,406	0.80
0.5	465	415	0.01	11,050	1.40
1.0	478	400	0.09	9696	1.18

3. Results and discussion

XRD patterns of monolithic PT and the PT/ZnO ceramic nanocomposites with 0.1, 0.5, 1.0, 3.0 and 5.0 wt% ZnO are shown in Fig. 2. In general, perovskite as a major PT phase is observable in all samples. No measurable change in *d*-spacing for the samples containing different ZnO contents was observed. All the peaks are ascribed to tetragonal $PbTiO_3$ (JCPDS file no. 6-452) [22]. Diffraction peaks of ZnO in the nanocomposites are not detectable probably because its amount was less than the XRD detection limits. However, when the content of ZnO nanowhiskers was more than 3.0 wt%, a considerable amount of Zn_2TiO_4 (▼) [23] was formed. This indicates that an evident chemical reaction occurred between PT and ZnO nanowhiskers. In the case of PZT/ZnO nanocomposites [13], it was shown that ZnO nanowhiskers were chemically inert to PZT at 1100 °C. In this work, ZnO nanowhiskers might act as a sin-

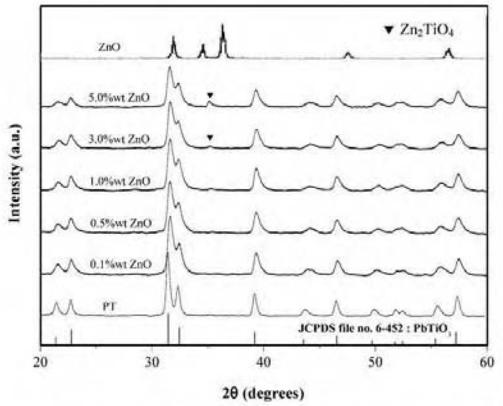

Fig. 2. XRD patterns of monolithic PT and PT/ZnO ceramics sintered at 1200 °C for 2 h.

tering aid so that samples with high ZnO contents (3.0 and 5.0 wt%) could be sintered at temperatures lower than 1200 °C. The presence of the secondary phase could be attributed to the high sintering temperature and a small degree of lead losses [24]. Moreover, by comparing these results with our previous work [17], it is found that SiC nanofibers are chemically inert to PT at identical sintering conditions.

Densities and tetragonality factors of the samples are listed in Table 1. The density values increased slightly with increasing content of ZnO nanowhiskers, from 0 to 0.5 wt%. Higher content of ZnO did not lead to further increase in density. Furthermore, the formation of oxygen vacancies due to Zn^{2+} ion substitution in perovskite structure is considered to be another reason for the sintering behavior of PT/ZnO nanocomposites [25]. Thus, the assumption that

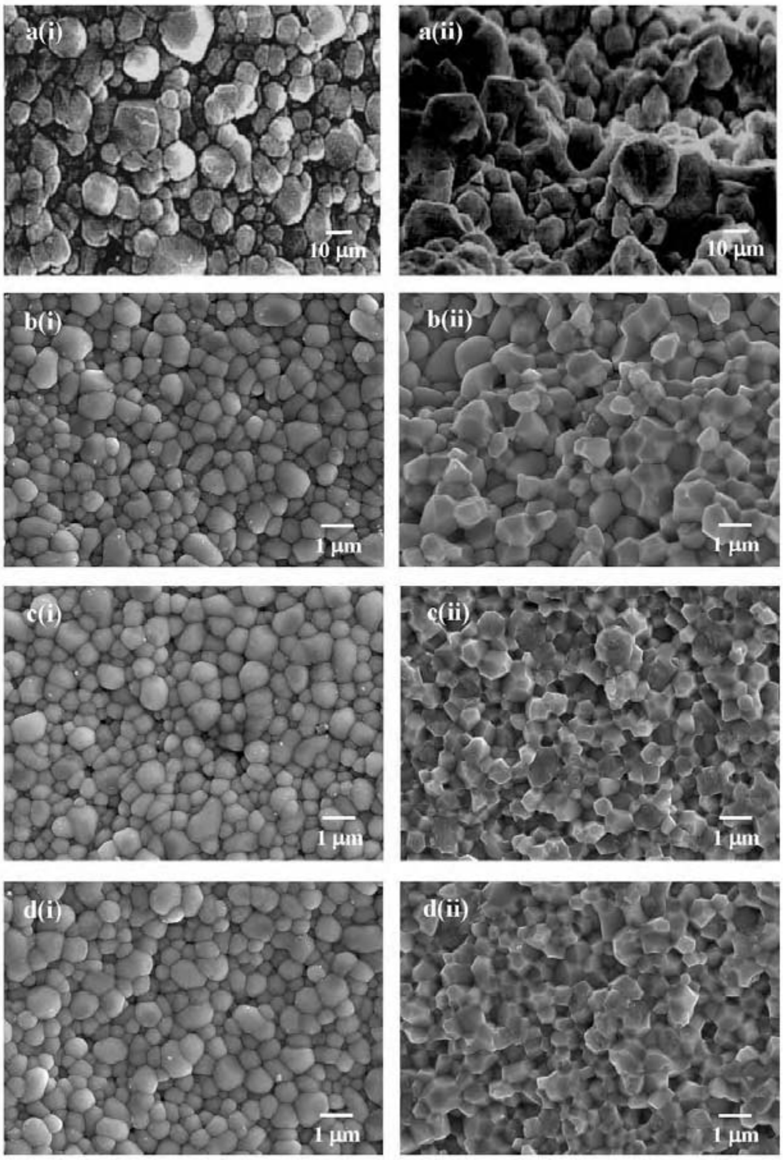

Fig. 3. Natural (i) and fractured (ii) surfaces of (a) monolithic PT and PT/ZnO ceramics with (b) 0.1 wt%, (c) 0.5 wt%, (d) 1 wt%, (e) 3 wt% and (f) 5 wt% of ZnO.

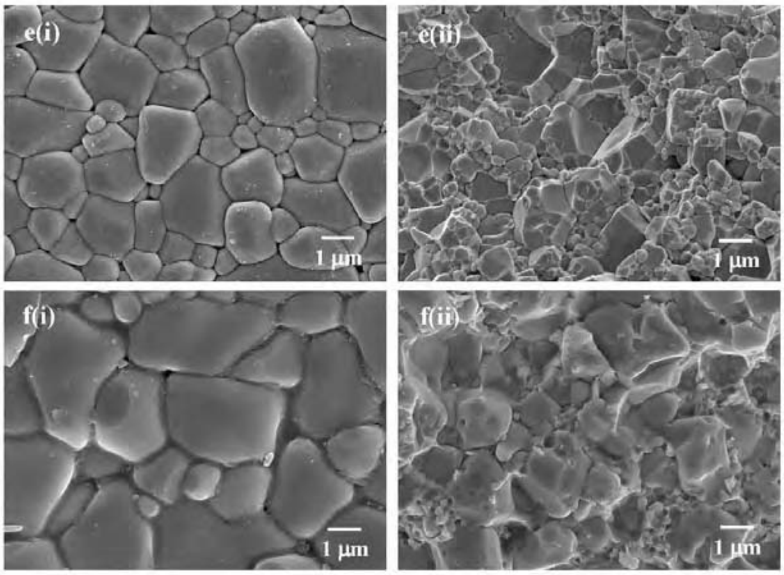

Fig. 3. (*Continued*).

oxygen vacancies accelerated mass transfer and densification – which was observed in other systems [26,27] – was valid in this system. This indicates that ZnO improved the sinterability of PT ceramics. Compared to pure PT ceramics, the composites have a smaller tetragonality factor, indicating a lower internal stress in these nanocomposites [16,17]. These data were estimated through the Cohen method [28]. One explanation for the decrease in tetragonality of the PT/ZnO could be the incorporation of Zn ions into the PT lattice during sintering [29]. Moreover, the results indicated that the addition of Zn^{2+} into the PT phase slightly reduced the lattice dimensions.

Microstructural features – natural (i) and fractured (ii) surfaces – of pure PT ceramics and PT/ZnO composites are displayed in Fig. 3. Pure PT ceramics have spherical grains and poor packing. In contrast, PT/ZnO nanocomposites possess equiaxed grains with good grain-packing. The average grain sizes were found to decrease significantly with increasing content of ZnO up to 3.0 wt%. It seems that ZnO nanowhiskers controlled grain boundary movement and limited grain growth of the PT matrix [17,29]. The samples with 3.0 and 5.0 wt% ZnO – Fig. 3 e(i) and f(i) – show clearly abnormal grain growth. These are important quantitative aspects of liquid-phase sintered microstructures. Moreover, in the sample with 5.0 wt% ZnO, a pronounced second phase is segregated at the grain boundaries, as shown in Fig. 3 f(i). The presence of these (second-phase) layers could be attributed to a liquid-phase formation during the sintering. Also, this same behavior can be noticed in other ceramic systems [30,31]. Thus, it can be concluded that ZnO acted as a sintering aid.

Generally, the fracture mode of samples with 0.1–1.0 wt% ZnO nanowhiskers was found to be predominantly of an intergranular-type, similar to that of monolithic PT ceramics because clear grain boundaries can be observed. In contrast [32,33], almost clean microstructures with highly uniform, dense, angular grain-packing are observed. On the other hand, with increasing ZnO content (more than 3.0 wt%), the samples have two grain size ranges, as shown in Fig. 3 e(ii) and f(ii). Movement of atoms is driven by differences in curvature between the particles in contact, probably because the particles have irregular shapes caused by milling [34]. Moreover, it is possible that the mass transport between several aggregated particles and the high anisotropy in the grain boundary energies induced the formation of compact polyhedral and irregular grains [34]. This indicates that two mechanisms are involved during sintering. Furthermore, it should be noted that the average grain sizes of all the PT/ZnO nanocomposites are smaller than the critical value of 3 μm [32,35], which gives rise to a volumetric percentage adequate to buffer the anisotropic stress caused by the phase transition [1]. The reduced grain size of the composites is considered to be responsible for the improvement of their mechanical properties [35,36].

Fig. 4 shows variations of dielectric constant and dielectric loss of the samples with different ZnO contents at various temperatures, as measured at 1 MHz. Dielectric constant (ε_r) and dielectric loss ($\tan\delta$) values at room temperature, and ferroelectric–paraelectric phase transition temperatures (T_C) of the samples are listed in Table 2. Generally they all behave as typical, normal ferroelectric materials [1]. A similar trend in dielectric values at T_C was also observed. From Fig. 4 b(i), it is evident that the addition of 0.1 wt% ZnO to PT leads to a drastic increase in dielectric constant. The dielectric constant of the composites then decreases slightly with further ZnO addition up to 1.0 wt%. However, the dielectric constant for all PT/ZnO composites appears to be higher than for pure PT ceramics. The higher dielectric constant of samples with small amounts of ZnO could be attributed mainly to the decrease in porosity. Moreover, it can be seen that with increasing ZnO content, T_C shifted towards lower temperatures. The shift of the phase transformation temperature in these PT/ZnO composites might be due to a relaxation of transformation-induced internal stress by the ZnO nanowhiskers dispersed in the PT matrix.

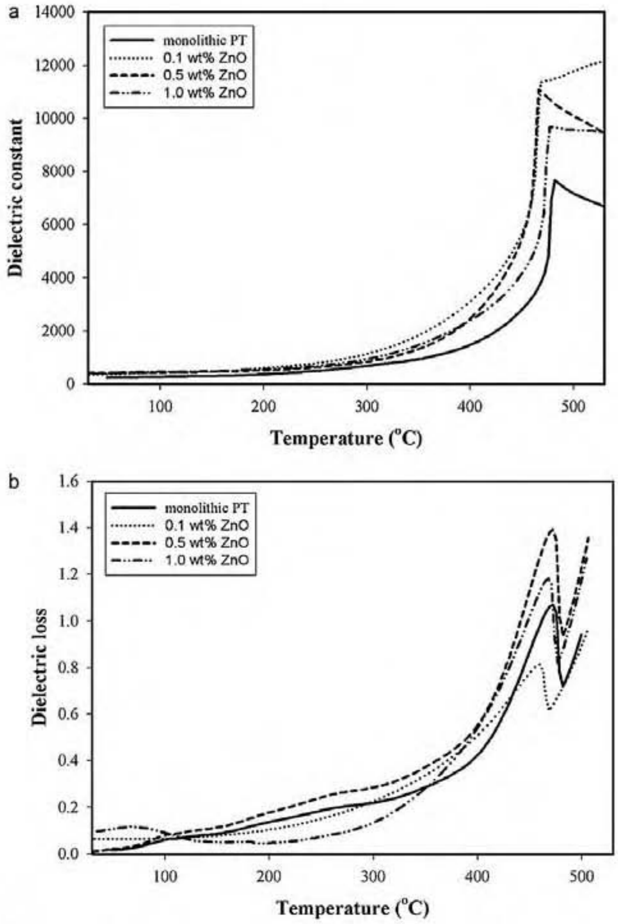

Fig. 4. Variation with temperature of (a) dielectric constant and (b) dielectric loss at 1 MHz of PT/ZnO ceramics with different ZnO contents.

4. Conclusions

$PbTiO_3$/ZnO ceramic composites can be fabricated using a simple and inexpensive solid-state reaction method. The materials had a tetragonal phase for all compositions. Moreover, the addition of ZnO nanowhiskers was found to significantly enhance densification, mechanical and dielectric properties of PT-based ceramics.

Acknowledgements

This work was supported by the Thailand Research Fund (TRF), the Commission on Higher Education (CHE), the National Nanotechnology Center (NANOTEC), and the Faculties of Science of Chiang Mai University and Maejo University. Also acknowledged for additional support are: the Industry/University Cooperative Research Center (I/UCRC) in HDD Component; the Faculty of Engineering, Khon Kaen University; and the National Electronics and Computer Technology Center (NECTEC) of the National Science and Technology Development Agency.

References

[1] A.J. Moulson, J.M. Herbert, Electroceramics, 2nd ed., Wiley, Chichester, 2003.
[2] E.C. Paris, M.F.C. Gurgel, T.M. Boschi, M.R. Joya, P.S. Pizani, A.G. Souza, E.R. Leite, J.A. Varela, E. Longo, J. Alloys Compd. 462 (2008) 157–163.
[3] R. Wongmaneerung, A. Rujiwatra, R. Yimnirun, S. Ananta, J. Alloys Compd. 475 (2009) 473–478.
[4] K. Ramam, M. Lopez, K. Chandramouli, J. Alloys Compd. 488 (2009) 211–216.
[5] C.C.M. Wu, M. Kahn, W. Moy, J. Am. Ceram. Soc. 79 (1996) 809–812.
[6] A.A. Yar, M. Montazerian, H. Abdizadeh, H.R. Baharvandi, J. Alloys Compd. 484 (2009) 400–404.
[7] M.H. Maneshian, M.K. Banerjee, J. Alloys Compd. 493 (2010) 613–618.
[8] S.K. Pandey, O.P. Thakur, D.K. Bhattacharya, C. Prakash, R. Chatterjee, J. Alloys Compd. 468 (2009) 356–359.
[9] Y. Wu, T. Feng, J. Alloys Compd. 491 (2010) 452–455.
[10] J. Yuan, D.W. Wang, H.B. Lin, Q.L. Zhao, D.Q. Zhang, M.S. Cao, J. Alloys Compd. 504 (2010) 123–128.
[11] M. Ipek, S. Zeytin, C. Bindal, J. Alloys Compd. 509 (2011) 486–489.
[12] F.X. Li, X.X. Yi, Z.Q. Cong, D.N. Fang, Mod. Phys. Lett. B 21 (2007) 1605–1610.
[13] J. Cui, G. Dong, Z. Yang, J. Du, J. Alloys Compd. 490 (2010) 353–357.
[14] H.J. Hwang, K. Watari, M. Sando, M. Toriyama, K. Niihara, J. Eur. Ceram. Soc. 19 (1999) 1179–1182.
[15] H.J. Hwang, T. Nagai, T. Ohji, M. Sando, M. Toriyama, K. Niihara, J. Am. Ceram. Soc. 81 (2005) 709–712.
[16] R. Wongmaneerung, R. Yimnirun, S. Ananta, Appl. Phys. A 86 (2007) 249–255.

[17] R. Wongmaneerung, P. Singjai, R. Yimnirun, S. Ananta, J. Alloys Compd. 475 (2009) 456–462.
[18] C. Ionascu, R. Schaller, Mater. Sci. Eng. A 442 (2006) 175–178.
[19] M.S. Cao, W. Zhou, X.L. Shi, Y.J. Chen, Appl. Phys. Lett. 91 (2007) 203110.
[20] S. Choopan, N. Hongsith, S. Tanunchai, T. Chairuangsri, P. Mangkorntong, N. Mangkorntong, J. Cryst. Growth 282 (2005) 365–369.
[21] H. Klug, L. Alexander, X-Ray Diffraction Procedures for Polycrystalline and Amorphous Materials, 2nd ed., Wiley, New York, 1974.
[22] JCPDS-ICDD Card No. 6-452, International Centre for Diffraction Data, Newtown Square, PA, 2000.
[23] S.K. Manik, S.K. Pradhan, Physica E 33 (2006) 69–76.
[24] R. Wongmaneerung, R. Yimnirun, S. Ananta, J. Electroceram. 21 (2007) 798–801.
[25] K. Vanheusden, W.L. Warren, C.H. Seager, D.R. Tallant, J.A. Voigt, B.E. Gnade, J. Appl. Phys. 79 (1996) 7983–7990.
[26] H.J. Hwang, M. Yasuoka, M. Sando, M. Toriyama, K. Niihara, J. Am. Ceram. Soc. 82 (2004) 2417–2422.
[27] P.H. Xiang, X.L. Dong, C.D. Feng, N. Zhong, J.K. Guo, Ceram. Int. 30 (2004) 765–772.
[28] B.D. Cullity, Elements of X-Ray Diffraction, 2nd ed., Addison Wesley, Sydney, 1978, p. 363.
[29] Y. Xu, A. Zangvil, A. Kerber, J. Eur. Ceram. Soc. 17 (1997) 921–928.
[30] M.L. Arefin, F. Raether, D. Dolejš, A. Klimera, Ceram. Int. 35 (2009) 3313–3320.
[31] P. Yongping, L. Yunhe, Y. Wenhu, J. Rare Earths 25 (2007) 167–170.
[32] A. Udomporn, K. Pengpat, S. Ananta, J. Eur. Ceram. Soc. 24 (2004) 185–188.
[33] R. Wongmaneerung, R. Yimnirun, S. Ananta, Appl. Phys. A 86 (2007) 2498–3255.
[34] M.N. Rahaman, Sintering of Ceramics, CRC Press/Taylor and Francis Group, Boca Raton, FL, 2008, pp. 55–106.
[35] L.B. Kong, W. Zhu, O.K. Tan, J. Mater. Sci. Lett. 19 (2000) 1963–1966.
[36] T. Suwannasiri, A. Safari, J. Am. Ceram. Soc. 76 (1993) 3155–3158.

Advanced Materials Research Vols. 194-196 (2011) pp 2046-2049
© (2011) Trans Tech Publications, Switzerland
doi:10.4028/www.scientific.net/AMR.194-196.2046

Surface Characterization of the Corundum-Route Lead Magnesium Niobate Ferroelectric Ceramics

La-ongnuan Srisombat[1,a], Rewadee Wongmaneerung[2,b],
Rattikorn Yimnirun[3,c] and Supon Ananta[4,d]

[1]Department of Chemistry, Faculty of Science, Chiang Mai University, Chiang Mai 50200 Thailand

[2]Department of Physics, Faculty of Science, Maejo University, Chiang Mai 50290 Thailand

[3]School of Physics, Institute of Science, Suranaree University of Technology, Nakhon Ratchasima 30000 Thailand

[4]Department of Physics, Faculty of Science, Chiang Mai University, Chiang Mai 50200 Thailand

[a,*]slaongnuan@yahoo.com, [b]re_nok@yahoo.com, [c]rattikornyimnirun@yahoo.com,
[d]suponananta@yahoo.com

Keywords: Lead Magnesium Niobate; X-ray Photoelectron Spectroscopy; Surface Analysis

Abstract. Perovskite relaxor ferroelectric PMN ceramics, Pb $(Mg_{1/3}Nb_{2/3}O_3)$, have been fabricated using a two-stage process employing a corundum-type $Mg_4Nb_2O_9$ as a key precursor. The 100% perovskite PMN ceramics was revealed by X-ray diffraction analysis. The SEM image of the PMN ceramic shows irregular shape PMN grains on the porous surface. The surface chemical composition of the PMN ceramics could be characterized by X-ray photoelectron microscopy technique. The XPS results indicate most of the elements consist of more than one chemical species. The important of XPS studies here can reveal small amount of species which could not detected by XRD.

Introduction

Ceramics based on the relaxor ferroelectric lead magnesium niobate, $Pb(Mg_{1/3}Nb_{2/3})O_3$, (PMN) perovskite are widely employed in microelectronics as multilayer capacitors, actuators, and components that operate via the induced piezoelectric effect [1-3]. Applications involving these materials vary with their mechanical, electrical, and piezoelectric properties, which depend on the composition and the nature of the defects in the sample. Several studies have focused on the cystal structure [4], microstructure [5], and electrical properties [6] of this material. Even though the previous study of the surface characteristics of the PMN ceramics prepared by columbite *B*-site precursor has been reported [7], the study of the surface characteristics of the PMN ceramics derived from corundum *B*-site precursor has not been studied. Thus, the aim of this work is to characterize phase composition, morphology and chemical composition of PMN ceramics especially at the surfaces by using a combination of several techniques including XRD, SEM, and XPS, respectively.

Experimental

Perovskite relaxor ferroelectric ceramics with general formula $Pb(Mg_{1/3}Nb_{2/3})O_3$ were fabricated by a similar methodology of *B*-site precursor mixed-oxide synthetic route, as reported earlier [8]. Corundum-type $Mg_4Nb_2O_9$ powders were first prepared by using magnesium oxide (MgO) and niobium oxide (Nb_2O_5), (Aldrich, 99% purity) as raw materials [9]. Pure phase of $Mg_4Nb_2O_9$ was then mixed with PbO via a rapid vibro-milling technique for 30 min in isopropanol, the mixtures were calcined at 950 °C for 1 h with heating/cooling rates of 30°C/min to generate PMN powders [10]. Ceramic fabrication was carried out by adding 3 wt% polyvinyl alcohol (PVA) binder, prior to pressing as pellets in a uniaxial die press. Green PMN pellets were placed inside double alumina crucibles and sintered in air at 1250 °C for 2 h with heating/cooling rates of 30°C/min. Phase formation, microstructure, and chemical composition of the sintered PMN ceramics were examined by using X-ray diffraction (XRD; Philips PW 1729 diffractometer), scanning electron microscopy (SEM; JEOL JSM-840A) and a PHI 5700 X-ray photoelectron spectrometer (XPS) equipped with PHI 04091 neutralizer, respectively.

Results and Discussion

X-ray diffraction pattern of the corundum-route PMN ceramic is given in Fig. 1, indicating the formation of a pure $Pb(Mg_{1/3}Nb_{2/3})O_3$ perovskite phase, which could be matched with JCPDS file no. 81-861, in agreement with previous works [5,8]. As-fired surface SEM micrograph of this corundum-route PMN ceramic is also shown in Fig. 2. In general, SEM micrograph of as-fired structure of this PMN ceramic shows highly porous and heterogeneous microstructure consisting of flaky and irregular-shaped grains. The PMN grains are different in shape with significant variation in size ranging from ~1-10 μm. It is believed that this high degree porosity could be attributed mainly to the effect of PbO volatilization particularly at the surface during high sintering temperature process, in agreement with literatures [5,8]. The surface morphology of this corundum-route PMN ceramic is significantly different from those of the typical columbite-route PMN ceramics [10].

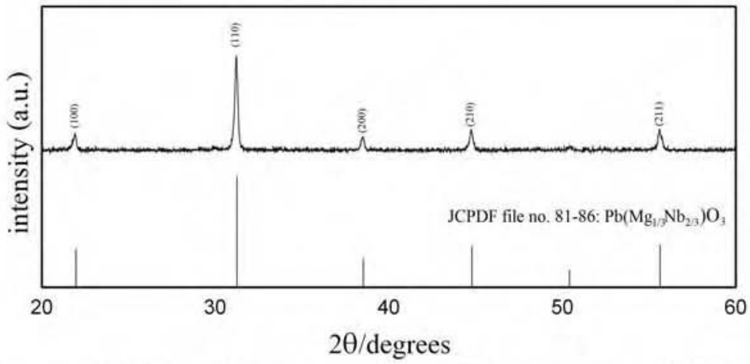

Fig. 1 Computerized JCPDS data-matching confirms the formation of cubic PMN phase in the corundum-route PMN ceramic.

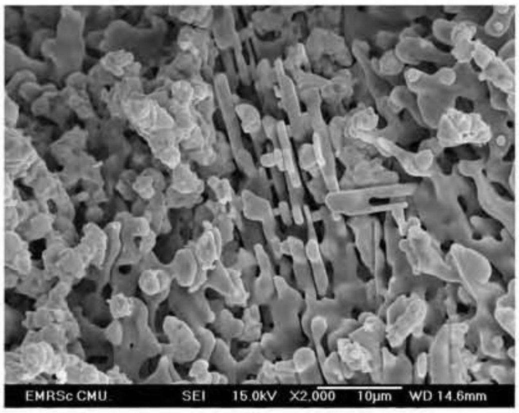

Fig. 2 SEM micrograph of as-fired surface of the corundum-route PMN ceramics

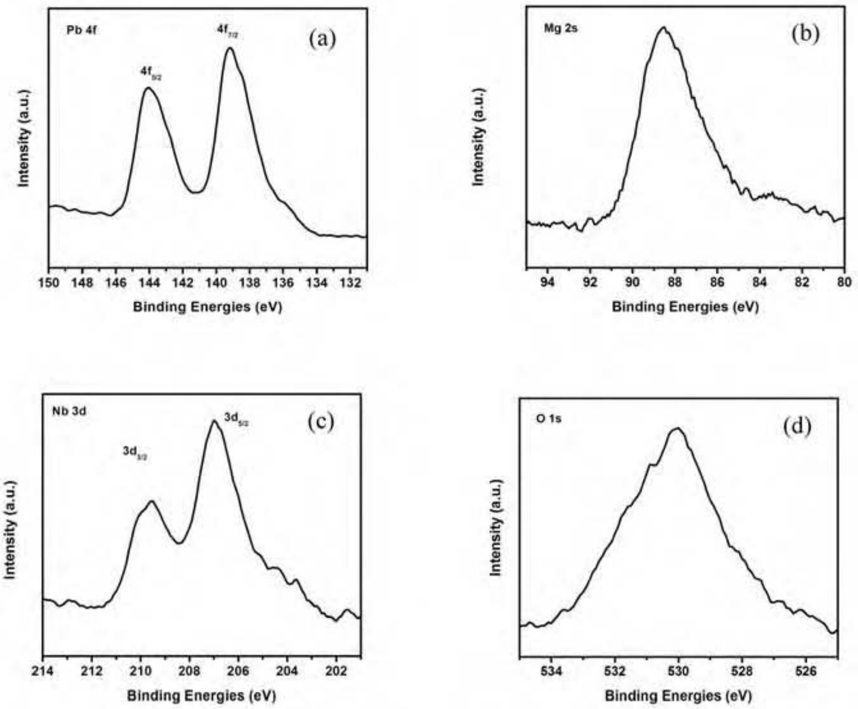

Fig. 3 The XPS spectra (a) Pb 4f, (b) Mg 2s, (c) Nb 3d, and (d) O 1s lines of the corundum-route PMN ceramics.

Wide energy range of XPS spectrum of the PMN ceramics shows all elementary compositions of the compound (data not shown). Fig. 3 shows the narrow-scan XPS spectra of Pb, Mg, Nb, and O core level, respectively. The XPS spectrum of Pb $4f_{7/2}$ of PMN (Fig. 3a) reveals a shoulder peak. This Pb $4f_{7/2}$ peak can be deconvoluted into two components. The first peak at ~138.2 eV can be assigned to Pb^{2+} in the perovskite structure [11,12], while the second peak at ~136.8 eV might due to Pb^0 which general found on the surface of ferroelectric samples reported in the literatures [13,14]. The Mg 2s peak of PMN (Fig. 3b) appear a broad and shouder peak indicating more than one components of Mg species presented in the samples. The Nb 3d peaks of the PMN caramic (Fig. 3c) are also broad and asymmetry peaks. Those peaks can be deconvolution into two components. The first component of at ~206.8 eV corresponds to Nb in the perovskite structure [7,15]. The second component at lower binding energy might attribute to unreacted Nb_2O_5 which reported by Singh *et al.* [16], or Nb^{4+} which generated by the reduction of Nb^{5+} caused by sputtering process. We here still could not identify exactly the component at lower binding energy, however, the XPS studies here can indicate small amount components which could not be detected by XRD. The narrow-scan of O 1s core level spectrum of the PMN ceramic in Fig. 3d shows a broad peak indicating more than one species of oxygen presented in the sample. The oxygen peak might be deconvoluted to several components ~527.3 eV, ~529.2 eV, ~530.8 eV and ~532.1 eV. The peak at ~529.2 eV usually assigned to oxygen in the perovskite lattice [17-20]. The other peak appears might be attributed to absorbed oxygen species as suggested by Xu *et al.* [21]

Summary

For the first time, the chemical composition of the perovskite relaxor ferroelectric PMN ceramics derived from a corundum B-site precursor route was investigated by using a combination of XRD, SEM and XPS techniques. Even though the XRD result indicates a pure perovskite phase, by using the XPS and SEM analysis reveals other components presented in the surface of the PMN ceramics. Our study here show that a single technique of XRD could not provide fully chemical information of the PMN ceramics.

Acknowledgements

This work was financially supported by the Thailand Research Fund (TRF), the Commission on Higher Education (CHE), and Chiang Mai University.

References

[1] A. J. Moulson and J. M. Herbert: *Electroceramics*: (Wiley, Chichester, 2003).

[2] G. H. Haertling: J. Am. Ceram. Soc. Vol. 82 (1999), p. 797.

[3] E. F. Alberta and A. S. Bhalla: J. Phys. Chem. Solids Vol. 63 (2002), p. 1759.

[4] E. Husson, L. Abello and A. Morell: Mater. Res. Vol 25(1990), p. 539.

[5] S. Ananta and N.W. Thomas: J. Eur. Ceram. Soc. Vol. 19 (1999), p. 2917.

[6] R. Yimnirun, S. Ananta and P. Laoratanakul: J. Eur. Ceram. Soc. Vol. 25 (2005), p. 3235.

[7] S. M. Gupta, A. R. Kulkarni, M. Vedpathak and S. K. Kulkarni: Mater. Sci. Eng., B Vol. B39 (1996), p. 34.

[8] R. Wongmaneerung, R. Yimnirun and S. Ananta: J. Alloys Compd. Vol. 477 (2009), p. 805.

[9] S. Ananta: Mater. Lett. Vol. 58 (2004), p. 2834.

[10]R. Wongmaneerung, T. Sarakonsri, R. Yimnirun and S. Ananta: Mater. Sci. Eng. B Vol. 132 (2006), p. 292.

[11]L. Srisombat, O. Khamman, R. Yimnirun, S. Ananta and T.R. Lee: Chiang Mai J. Sci. Vol. 36 (2009), p.69.

[12] A. Molak, E. Talik, M. Kruczek, M. Paluch, A. Ratuszna and Z. Ujma: Mater. Sci. Eng., B Vol. 128 (2006), p. 16.

[13] V.R. Mastelaro, P.N. Lisbao-Filho, P.P. Neves, W.H. Schreiner, P.A.P. Nascente and J.A. Eiras: J. Electron. Spectrosc. Relat. Phenom. Vol. 156-158 (2007), p. 476.

[14] S. Bhaskar, S.B. Majunder and E.R. Katiyar: J. Am. Ceram. Soc. Vol. 87 (2004), p.384.

[15]L. Srisombat, O. Khamman, R. Yimmirun, S. Ananta and T.R. Lee: Key Eng. Mater. Vol. 421-422 (2010), p. 415.

[16]P. Singh, B.J. Brandenburg, C.P. Sebastian, D. Kumar and O. Parkash: Mater. Res. Bull. Vol. 42 (2008), p. 2078.

[17]Q.N. Pham, C. Bohnke and O. Bohnke: Surf. Sci. Vol. 572 (2004), p. 375.

[18]Z. Xia, Q. Li and M. Cheng: Cryst. Res. Technol. Vol. 42 (2007), p. 511.

[19]C. R. Cho: Cryst. Res. Technol. Vol. 35 (2000), p. 77.

[20]C. J. Lu, A.X. Kuang and G. Y. Huang: J.Appl. Phys. Vol. 80 (1996), p. 202.

[21]Q. Xu, D. Huang, W. Chen, H. Wang, Bi Wang and R. Yuan: Appl. Surf. Sci. Vol. 228 (2004), p 110.

2. manuscript ที่ได้จัดส่งวารสาร Journal of materials processing technology

Microstructure and dielectric properties of two-stage sintered PMN-PT ceramics prepared by corundum route

R. Wongmaneerung[a*], R. Yimnirun[b], S. Ananta

[a]Faculty of Science, Maejo University, Chiang Mai 50290, Thailand

[b]School of Physics, Institute of Science, Suranaree University of Technology, Nakhon Ratchasima 30000, Thailand

[c]Department of Physics and Materials Science, Faculty of Science, Chiang Mai University, Chiang Mai 50200, Thailand

ABSTRACT

A two-stage sintering technique, which began with an initial heating at lower temperature and followed by higher temperature sintering, was employed in the production of PMN-PT ceramics prepared by a corundum route. Effects of designed sintering conditions on phase formation, microstructure and dielectric properties of the samples were characterized via X-ray diffraction (XRD), scanning electron microscope (SEM) and dielectric measurement, respectively. The types of phase present are found to depend upon sintering conditions. The grains are similar in shape. Micrograph shows a few pores at triple points. In addition, it is seen that the PMN-PT samples also have an intergranular fracture mechanism. In connection with the dielectric properties, a dependence of the dielectric constant and dielectric loss on sintering scheme is observed. Moreover, this work demonstrated that under suitable two-stage sintering schemes, perovskite PMN-PT ceramics can be successfully achieved with better dielectric properties than those of ceramics from a conventional method.

Keywords: *Lead magnesium niobate-lead titanate; perovskite; two-stage sintering; dielectric properties*

1. Introduction

In relaxor ferroelectrics, such as several perovskite-type compounds, lead magnesium niobate (PMN), lead strontium titanate (PST) and lead zinc niobate (PZN) attract considerable interest owing to rich diversity of their physical properties and possible applications in various technological schemes (Moulson and Herbert, 2003 and Uchino, 2000). One of the difficulties with most composition containing lead and niobate is a tendency of the formation of pyrochlore-type rather than perovskite-type structures with lower relative permittivity values (Moulson and Herbert, 2003). The addition of lead titanate (PT) helps to improve the yield of perovskite phase. Moreover, these compositions exhibit excellent machinability and high dielectric properties and have been applied in area such as multilayer capacitors and electrostrictive actuators (Cross, 1996 and Guha, 2003).

From the point of view of these applications, the ideal materials would provide a high dielectric constant over the operational temperature range. The main problem to the commercial exploitation of lead-based perovskite arises from processing difficulties, corresponding to PbO vapor during sintering and low density. Swartz et al., 1984 as well as Guha et al., 1988, Wongmaneerung et al., 2008 have been made to enhance processing techniques to develop materials with properties approaching application requirement. Besides using these methods, the modified sintering technique is one way to help improve ceramic densification. This technique is a complicated process of microstructure evolution, with the main outcome being porosity elimination. In practice, sintering is a crucial stage which can significantly affect the densification and the dielectric properties of the ceramics more strongly than the choice of reaction precursors. Moreover, in past years, only a few works on the preparation of PMN powders by using a corundum $Mg_4Nb_2O_9$ precursor have been reported. Joy and Sreedhar (1997) reported that for the synthesis of the relaxor type PMN, $Mg_4Nb_2O_9$ is a better precursor than the columbite $MgNb_2O_6$ presented by Swartz et al. (1984) to get rid of the unwanted pyrochlore phase from the final perovskite.

According to Wongmaneerung et al. (2009), a combination between the *B*-site precursor and the two-stage sintering technique has been proposed to achieve densification of PMN ceramics. Furthermore, this method has been successfully applied in production of lead titanate (Wongmaneerung et al., 2009). However, no work has been done on the investigation of the use of two-stage sintering PMN-PT ceramic. Therefore, in the present study, a two-stage sintering method has been attempted to fabricate the relaxor perovskite PMN-PT ceramics. The influence of doubly sintering conditions on phase formation, microstructure and dielectric properties of the ceramics is investigated.

2. Experimental procedure

The (1-x)PMN-xPT powders with $x = 0.1$-0.5 were prepared using the corundum precursor route, and their processing details were described by Wongmaneerung et al. (2007, 2009). In the mixing, the calculated relevant proportions of constituents were weighed, suspended in ethanol, and intimately mixed in a ball-mill with grinding media. After drying, the (1-x)PMN-xPT powders were obtained at 850 ^oC for 2 h. After re-milling, ceramic fabrication was achieved by adding 3 wt% polyvinyl alcohol (PVA) binder and sample pellets were obtained by uniaxial pressing and the binder was burned out at 500 ^oC for 1 h prior to sintering. The green bodies were sintered in a sealed system. The samples were surrounded with $PbTiO_3$ to reduce loss of volatile components. Two sets of the first sintering temperature (T_1) were assigned for the two-stage sintering case: 1100 and 1150 ^oC for 2 h. The second sintering temperature (T_2) at 1200 ^oC for 2 h was carried out for each case.

The phase structures for all samples were examined by an XRD, using Cu Kα radiation. The densities of all samples were determined using the Archimedes' method. Weight loss of all sintered samples was measured from the weight change (Δw) with respect to the original weight (w_o) before sintering. The as-sintered and fracture surfaces of sintered pellets were determined by SEM analysis. Dielectric measurement was operated on an automated system, composed of a HP4824A Precision LCR meter, a Delta 9023 automated temperature-controlling box and computer automated control program. Five frequencies (1 Hz, 1 kHz, 10 kHz, 100 kHz and 1 MHz) were selected to measure the dielectric constant and loss and the temperature ranges were -50 to 200 ^{o}C.

3. Results and discussion

To ensure the quality of the perovskite phase, the (1-*x*)PMN-*x*PT samples were X-rayed to check the relative amount of perovskite formed. Fig. 1(a) and (b) show the XRD profiles of compositions with x = 0.1-0.5 sintered at 1100/1200 ^{o}C and 1150/1200 ^{o}C, respectively and reveal that no pyrochlore phase exists. The {111} and {200} reflection lines were found to become broader or split with PT increasing, indicating that a phase transition occurs. Moreover, a careful observation showed only a pseudo-cubic symmetry at low PT concentration, in agreement with Suh et al. (2002) as well as Fengbing et al. (2004). By comparison to PMN-PT ceramics sintered at 1150/1200 ^{o}C, the XRD patterns of these samples were found to split at lower PT value as shown in Fig. 1(a) and (b). One possible reason could be due to the higher first temperature (T_1 = 1150 ^{o}C) leading to peak splitting. This is probably because the energy is high enough to make the reaction between PMN and PT and induce the PT phase into PMN phase more easily than using low first temperature. The XRD results clearly show that, in general, the different sintering conditions used for preparing PMN-PT ceramics gave rise to a different phase formation in this material.

Table 1 also presents the relative density, weight loss and grain size data of the two-stage sintered PMN-PT samples compared with conventional case that was completed by Wongmaneerung et al. (2009). The two-stage sintered PMN-PT densification was found to increase with first firing temperature and PT concentration, which could be due to lower melting point of PT compared to PMN (Udomporn, 2004). Density values between 7.62 and 7.94 g/cm^3 were obtained after sintering at 1100/1200 ^{o}C and 1150/1200 ^{o}C, respectively. Weight losses of all PMN-PT ceramics during sintering procedure can be thought of as a measure of the degree of PbO volatilization. This was analyzed by recording the weight before and after sintering procedure. In general, the weight loss increases with sintering temperature. Furthermore, in Table 1, it can be seen that grain sizes of PMN-PT ceramics sintered with two-stage sintering method are slightly larger than those obtained in conventional sintering technique. This observation shows that the energy from two-stage sintering temperature was used for accelerate the grain growth which is different from Wang et al. (2006).

As sintered and fracture surface SEM micrographs of 0.9PMN-0.1PT and 0.7PMN-0.3PT samples doubly sintered with different schemes are shown in Fig. 2 and 3, respectively. Cleary, the free surface microstructure of these samples is significantly different from those of the normal sintering (Wongmaneerung, 2009). From Fig. 2a(i), it can be noted that the microstructure consists of small matrix grains of about 0.3 µm and abnormally growth grains of about 3.7 µm. In this respect, it has occurred at T_1 of about 1100 ^{o}C due to the resultant acceleration in material transfer as observed by Matsuo and Sasaki (1971), Lee et al. (2000). Other possible reason is small matrix grains can be inhibited by the presence of second phase inclusion (Lee and Rainforth, 1994) such as MgO-rich phase as shown in Fig. 2a(ii). Therefore, grain growth is suppressed during the sintering process similar to the results observed by Wongmaneerung, 2009. According to Chung et al. (2002), Seo and Yoon (2005), it is possible that small amount of MgO is dissolved in the PbO-rich liquid or PMN-PT at high firing temperature, and its segregation at the grain-liquid interface and grain boundary may have made their step energies finite and hence made them sufficiently singular to cause abnormal grain growth. It was recognized that the XRD data alone could neither confirm nor rule out the presence of MgO because the high intensity XRD peak of MgO at d200 = 2.106 Å is almost overlapped by the perovskite PMN peak at d200 = 2.03 Å (Guha, 1999). However, to answer this question, the TEM technique can be used to examine the crystallographic orientation of the grain. When the 0.9PMN-0.1PT powder compact was sintered at 1150/1200 ^{o}C (Fig. 2b(i) and (ii)), the fine matrix grains were completely replaced by a new set of abnormally grown coarse grains. It can be seen that a high degree of porous surface is occurred and can be explained by PbO vaporization at high temperature. However, there is no presence of pores in fracture surface (Fig. 2b(ii)). Furthermore, Fig. 2 a(ii) and b(ii) show the fracture surface of 0.9PMN-0.1PT sintered at 1100/1200 ^{o}C and 1150/1200 ^{o}C, respectively. It can be seen that the form of small dark spherical particles (MgO phase) is randomly distributed in the solid solution matrix. The presence of MgO phase indicates their poor homogeneity due to the limitation of a mixed oxide processing. MgO inclusions correspond to dark particles, which can be found on the surfaces of some PMN-PT grains as shown in Fig. 3. Their corresponding EDX spectra are given in Fig. 4. It is to be noted that the characteristic morphology of MgO dispersed in PMN grains is consistent with previous work by Guha [23]. According to TEM observation by Goo et al. (1986), MgO tends to be segregated in the PMN grains as submicrometer inclusions and this segregation leads to a shortage of MgO on the whole, a situation liable to affect the formation of pyrochlore phase. By comparison between 0.9PMN-0.1PT and 0.7PMN-0.3PT samples sintered at the same temperature, the fracture mode of 0.9PMN-0.1PT ceramics is an intergranular because the clear grain boundaries can be observed. On the other hand, with increasing PT content, the grain boundary in the fracture surface became obscure as shown in Fig. 3 a(ii) and b(ii), and the fracture changed from intergranular to transgranular surface. The experimental work carried out here suggests that complex perovskite (*1-x*)PMN-*x*PT ceramics with a high degree of grain packing microstructures can be achieved by sintering powders derived from the *B*-site ($Mg_4Nb_2O_9$) precursor method.

Dielectric properties of 0.9PMN-0.1PT and 0.7PMN-0.3PT ceramics doubly sintered at various conditions were measured at frequencies between 100 Hz and 1 MHz in the temperature from -50 to 200 ^{o}C as shown in Fig. 5 and 6, respectively. In general, the typical relaxor behavior (Moulson, 2003) with the characteristics dispersive frequency dependence of the dielectric maxima has been observed in 0.9PMN-0.1PT. The values of maxima dielectric constant (ε_{max}) with different frequencies at $T = T_m$ for all samples were shown in Table 2, where T_m is the character temperature when ε reaches maximum. Fig. 5(a) and (b) shows a comparison of the dielectric of 0.9PMN-0.1PT ceramics two-stage sintered at 1100/1200 ^oC and 1150/1200 ^oC. It is easily found that the maxima dielectric constant versus temperature plots increase noticeably with increase in the first sintering temperature. Similar trend is also observed for T_m and $\tan\delta_m$. Moreover, the maximum of the dielectric constant decreases with increasing frequency, while that of the dielectric loss increases. Unlike the normal ferroelectric, the dielectric behavior of 0.9PMN-0.1PT ceramics cannot be described by the Curie-Weiss law equation. Further increase in PT concentration lead to more observable normal ferroelectric behavior because PT is intrinsically a normal ferroelectric according to Park and Shrout (1997). More interestingly, the 0.9PMN-0.1PT sample sintered at 1100/1200 ^oC showed one broad peak, whereas the 0.9PMN-0.1PT sample sintered at 1150/1200 ^oC had two peaks. One peak, at 30 ^oC, was stronger in intensity, and originated from the pure 0.9PMN-0.1PT solid solution grain core; the second, at 50 ^oC, caused by the chemical heterogeneity in the grain shell and gradient regions as the same results was observed by Park and Kim (1997). Furthermore, this behavior can be cause by the two-stage sintering mechanism. Even though exact mechanism of the dielectric behavior observed here is not well established and was not clearly observed by SEM to support the core-shell concept. In future work, HRTEM and Synchrotron techniques should be used to determine exact structure. For instance, the dielectric properties of 0.7PMN-0.3PT ceramics sintered at 1100/1200 ^oC and 1150/1200 ^oC (as displayed in Fig. 6(a) and (b)) exhibit a mixture of both normal and relaxor characteristics, in which the transition temperature is not shifted as much as for 0.9PMN-0.1PT samples. According to Noheda et al. (2002), Politova et al. (2003), it should be noted that 0.7PMN-0.3PT ceramic is close to MPB of the PMN-PT system. Therefore, its structural symmetry is a mixture of pseudo-cubic and tetragonal. More interestingly, it can be seen that there is a small broadening peak occurring at room temperature in 0.7PMN-0.3PT samples sintered at both case. Shrout et al. (1990) attributed similar dielectric anomalies to the rhombohedral to tetragonal phase transition in sample of lower Ti composition (30-35% PT) and a slight curvature in the MPB. Since the densities of the two ceramics are slightly different, this indicates that density could be the controlling factor for such observation. Besides higher density, the presence of MgO is one reason to enhancement of the dielectric constant of PMN-PT ceramics, as also observed by Lu and Lee (1995).

4. Conclusions

The potential of a combination between the B-site precursor and the two-stage sintering technique has been proposed to achieve dense and pure perovskite PMN-PT relaxor ceramics. They possess very high dielectric constants and fundamental dielectric properties which can be greatly varied by composition and sintering condition. This work demonstrated that two-stage sintering can effectively suppress the grain growth in PMN-PT system.

Acknowledgements

This work was supported by the Thailand Research Fund (TRF), Commission on Higher Education (CHE), and the Faculty of Science of Maejo University.

References

Chung, U.J., Park, J.K., Hwang, N.M., Lee, H.Y., Kim, D.Y., 2002. Effect of grain coalescence on the abnormal grain growth of $Pb(Mg_{1/3}Nb_{2/3})O_3$ 35 mol% $PbTiO_3$ ceramics. J. Am. Ceram. Soc. 85, 965–968.

Cross, L.E., 1996. Ferroelectric Ceramics: Materials and Applications Issues; in Ceramic Transactions, eds. Nair K. M. and Shukla V. N., Amercian Ceramic Society, Ohio, Westerville.

Fengbing, S., Qiang, L., Haisheng, Z., Chunhong, L., Shixi, Z., Dezhong, S., 2004. Phase formation and transitions in the lead magnesium niobate-lead titanate system. Mater. Chem. Phys. 83, 135–139.

Goo, E., Yamamoto, T., Okazaki, K., 1986. Microstructure of lead-magnesium niobate ceramics. J. Am. Ceram. Soc. 69, C188–C190.

Guha, J. P., 1999. Reaction chemistry and subsolidus phase equilibria in lead-based relaxor systems: Part I Formation and stability of the perovskite and pyrochlore compounds in the system PbO-MgO-Nb_2O_5. J. Mater. Sci. 85, 4985–4994.

Guha, J. P., 2003. Effect of compositional modifications on microstructure development and dielectric properties of Pb $(Mg_{1/3}Nb_{2/3})O_3$-$PbTiO_3$ solid solutions. J. Eur. Ceram. Soc. 23, 133–139.

Guha, J. P., Hong, D.J., Anderson, H.U., 1988. Effect of excess PbO on the sintering characteristics and dielectric properties of $Pb(Mg_{1/3}Nb_{2/3})O_3$–$PbTiO_3$ based ceramics. J. Am. Ceram. Soc. 71, C152–C154.

Joy, P.A., Sreedhar, K., 1997. Formation of lead magnesium niobate perovskite from niobate precursors having varying magnesium content. J. Am. Ceram. Soc. 80, 770–772.

Lee, H.Y., Kim, J.S., Hwang, N.M., Kim, D.Y., 2000. Effect of sintering temperature on the secondary abnormal grain growth of $BaTiO_3$. J. Eur. Ceram. Soc. 20, 731–737.

Lee, W.E., Rainforth, W.M., 1994. Book of Microstructure, Chapman & Hall, London.

Lu, C.H., Lee, J.T., 1995. Influence of Columbite $MgNb_2O_6$ on the perovskite formation and microstructure of $Pb(Mg_{1/3}Nb_{2/3})O_3$ ceramics. J. Ceram. Soc. Jpn. 103, 1122–1128.

Lu, C.H., Yang, H.S., 2001. Development of fast formation process for synthesizing submicron lead magnesium niobate perovskite powder. Mater. Sci. Eng. B 84, 159–162.

Matsuo, Y., Sasaki, H., 1971. Exaggerated grain growth in liquid-phase sintering of $BaTiO_3$. J. Am. Ceram. Soc. 54, 471.

Moulson, A.J., Herbert, J.M., 2003. Electroceramics, second ed. Wiley, Chichester.

Noheda, B., Cox, D.E., Shirane, G., 2002. Phase diagram of the ferroelectric relaxor $(1-x)PbMg_{1/3}Nb_{2/3}O_3$-$xPbTiO_3$. Phys. Rev. B 66, 054104–05413.

Park, S.E., Shrout, T.R., 1997. Relaxor based ferroelectric single crystals for electro-mechanical actuators. Mater. Res. Innov. 1, 20–25.

Park, Y., Kim, H.G., 1997. Dielectric temperature characteristics of cerium-modified barium titanate based ceramics with core-shell grain structure. J. Am. Ceram. Soc. 80, 106–112.

Politova, E.D., Abdulova, A.S., Kaleva, G.M., Shvartsman, V.V., 2003. Processing, dielectric and piezoelectric properties of the $PbTiO_3$-Based Ceramics. Ferroelectrics 285, 251–257.

Seo, C.E., Yoon, D.Y., 2005. The effect of MgO addition on grain growth in PMN–35PT. J. Am. Ceram. Soc. 88, 963–967.

Shrout, T.R., Chang, Z.P., Kim, N., Markgraf, S., 1990. Dielectric behavior of single crystals near the $(1-x)Pb(Mg_{1/3}Nb_{2/3})O_3$–$xPbTiO_3$ morphotropic phase boundary. Ferroelect. Lett. 12, 63–69.

Suh, D.H., Lee, D.H., Kim, N. K., 2002. Phase developments and dielectric/ferroelectric responses in the PMN–PT system. J. Eur. Ceram. Soc. 22, 219–223.

Swartz, S.L., Shrout, T.R., Schulze, W.A., Cross, L.E., 1984. Dielectric properties of lead magnesium niobate ceramics. J. Am. Ceram. Soc. 67, 311–314.

Uchino, K., 2000. Ferroelectric Devices, Marcel Dekker, New York.

Udomporn, A., Ananta, S., 2004. Effect of calcination condition on phase formation and particle size of lead titanate powders synthesized by the solid-state reaction. Mater. Lett. 58, 1154–1159.

Wang, X.-H., Chen, P.-L., Chen, I.-W., 2006. Two-step sintering of ceramics with constant grain-size, I. Y_2O_3. J. Am. Ceram. Soc. 89, 431–437.

Wongmaneerung, R., Sarakonsri, T., Yimnirun, R., Ananta, S., 2006. Effects of magnesium niobate precursor and calcination condition on phase formation and morphology of lead magnesium niobate powders. Mater. Sci. Eng. B 130, 246–253.

Wongmaneerung, R., Yimnirun, R., Ananta, S., 2007. Effects of sintering condition on phase formation, microstructure and dielectric properties of lead titanate ceramics. Appl. Phys. A 86, 249–255.

Wongmaneerung, R., Yimnirun, R., Ananta, S., 2009. Effect of two-stage sintering on phase formation, microstructure and dielectric properties of perovskite PMN ceramics derived from a corundum $Mg_4Nb_2O_9$ precursor. Mater. Chem. Phys. 114, 569–575.

Wongmaneerung, R., Yimnirun, R., Ananta, S., 2009. Synthesis and electrical properties of $Pb(Mg_{1/3}Nb_{2/3})O_3$–$PbTiO_3$ ceramics. Curr. Appl. Phys. 9, 268–273.

List of Table Captions

Table 1 Physical properties of (*1*-*x*)PMN-*x*PT ceramics from two-stage sintering conditions.

Table 2 Dielectric properties of (*1*-*x*)PMN-*x*PT ceramics.

List of Figure Captions

Fig. 1 XRD patterns of (*1*-*x*)PMN-*x*PT ceramics sintered at (a) 1100/1200 ^{o}C and (b) 1150/1200 ^{o}C.

Fig. 2 SEM micrographs of 0.9PMN-0.1PT ceramics sintered at (a) 1100/1200 ^{o}C and (b) 1150/1200 ^{o}C.

Fig. 3 SEM micrographs of 0.7PMN-0.3PT ceramics sintered at (a) 1100/1200 ^{o}C and (b) 1150/1200 ^{o}C.

Fig. 4 Representative EDX spectra obtained from the dark particles (arrowed in Fig. 3a (ii)) exist on the fracture of 0.9PMN-0.1PT grains (some spectra indexed as Au come from coated electrode).

Fig. 5 Temperature and frequency dependences of dielectric properties of 0.9PMN-0.1PT ceramics sintered at (a) 1100/1200 ^{o}C and (b) 1150/1200 ^{o}C.

Fig. 6 Temperature and frequency dependences of dielectric properties of 0.7PMN-0.3PT ceramics sintered at (a) 1100/1200 ^{o}C and (b) 1150/1200 ^{o}C.

Table 1

T_1/T_2 (°C for 2 h)	**Composition (x)**	**Density[a] (g/cm^3)**	**Weight loss[b] (%)**	**Grain-size[c] (μm)**
1100/1200	0.1	7.62	8.54	0.31-3.73
	0.2	7.66	8.32	0.42-3.80
	0.3	7.84	8.41	0.45-3.82
	0.4	7.81	8.65	0.53-3.98
	0.5	7.86	8.60	0.55-4.12
1150/1200	0.1	7.79	9.63	0.73-4.01
	0.2	7.73	9.55	0.96-4.01
	0.3	7.85	9.62	1.46-4.12
	0.4	7.90	9.43	1.55-5.76
	0.5	7.94	9.48	3.01-8.32
1240 [13]	0.1	7.98	12.75	0.42-3.66
	0.2	7.94	12.54	0.44-3.02
	0.3	7.86	12.23	0.41-2.80
1220 [13]	0.4	7.83	12.37	0.41-3.45
	0.5	7.78	12.46	0.48-3.72

[a] The estimated precision of the density is ± 0.05 g/cm^3

[b] The estimated precision of the weight loss is ± 0.1%.

[c] The estimated precision of the grain size is ± 0.05 m

Table 2

T_1/T_2	**Composition**	**T_m**	**Dielectric Properties[a]**	
(°C for 2 h)	**(x)**	**(°C)**	**$\varepsilon_{r,max}$**	**tan δ_{max}**
1100/1200	0.1	26.2	14750	0.08
	0.3	160	12380	0.18
1150/1200	0.1	30	23245	0.06
	0.3	162	18745	0.08

[a] Measured at 25 °C and 1 kHz

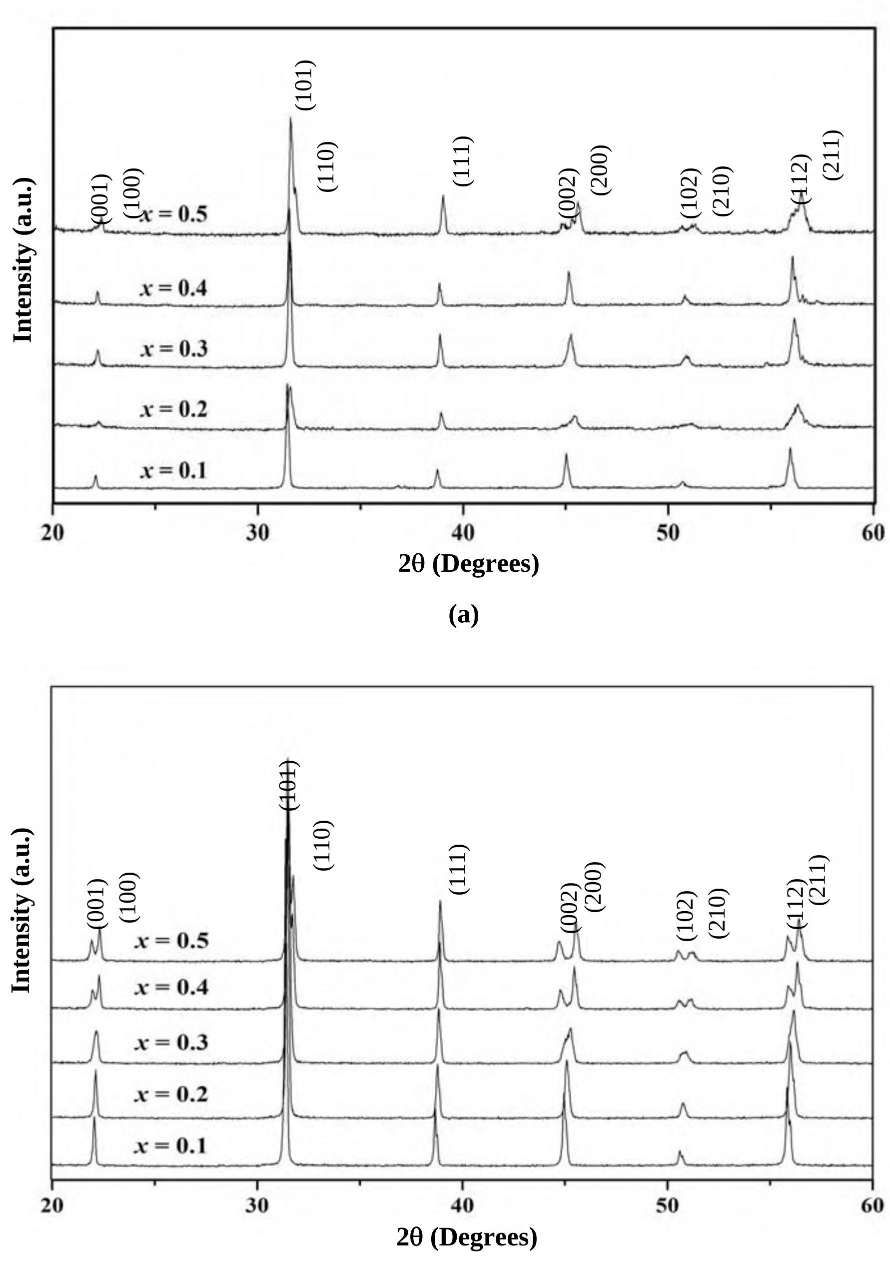
Intensity (a.u.)
(001)
(100)
(101)
(110)
(111)
(002)
(200)
(102)
(210)
(112)
(211)
x = 0.5
x = 0.4
x = 0.3
x = 0.2
x = 0.1
20
30
40
50
60
2θ (Degrees)
Intensity (a.u.)
(001)
(100)
(101)
(110)
(111)
(002)
(200)
(102)
(210)
(112)
(211)
x = 0.5
x = 0.4
x = 0.3
x = 0.2
x = 0.1
20
30
40
50
60
2θ (Degrees)

(a)

(b)

Fig. 1

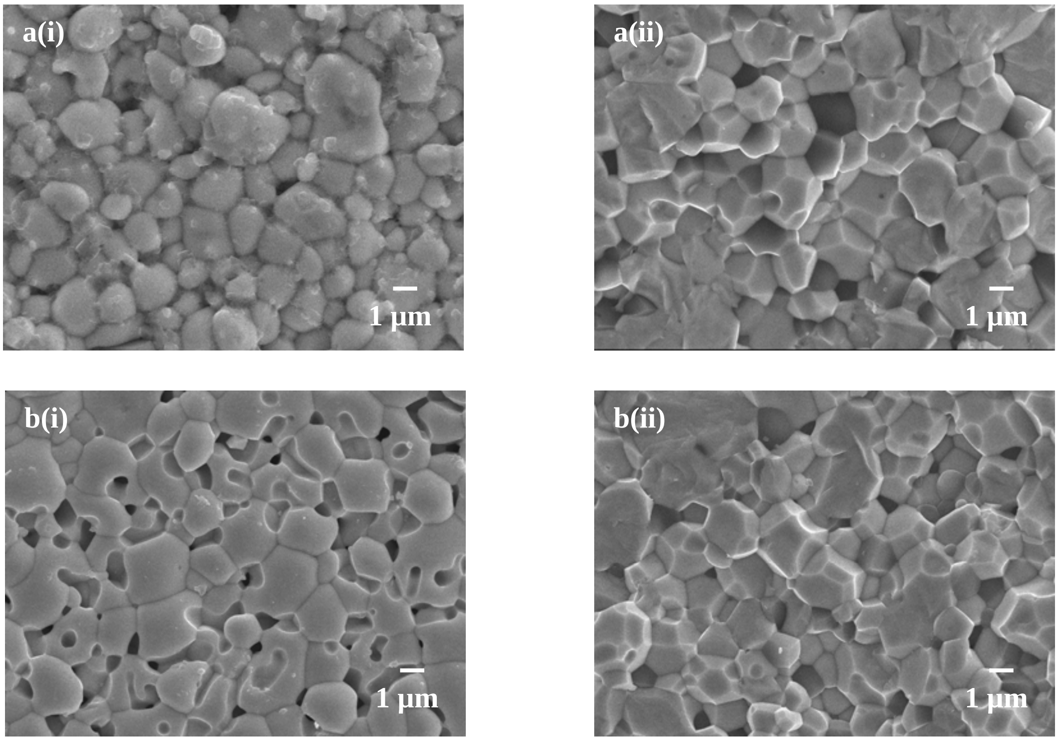

Fig. 2

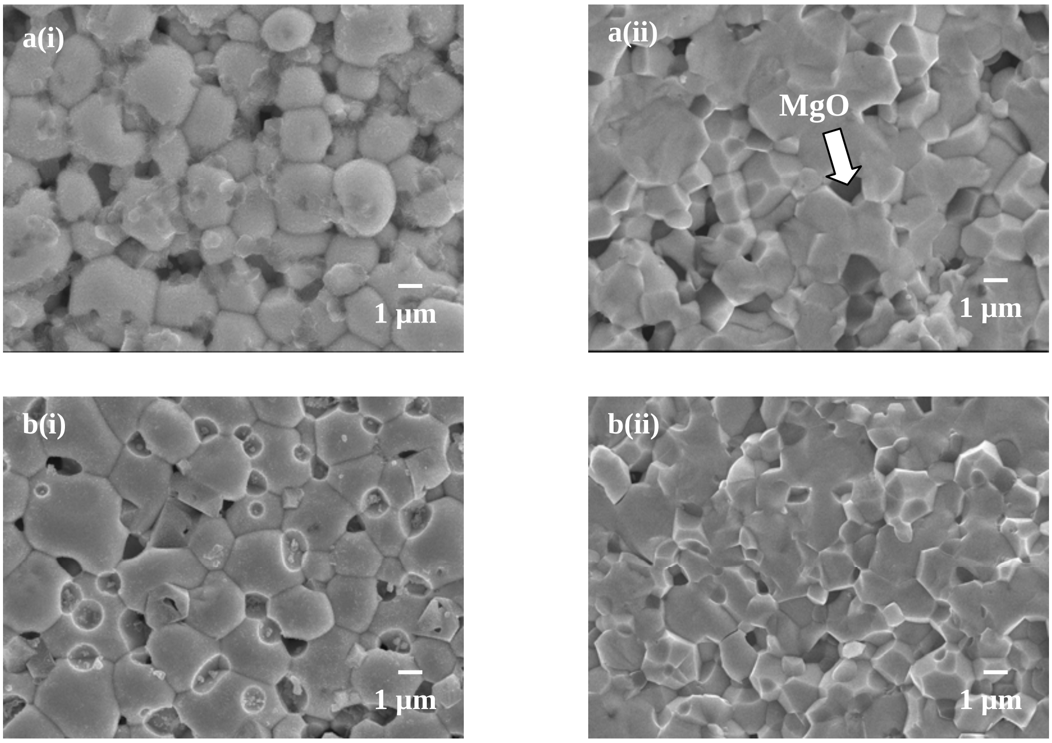

Fig. 3

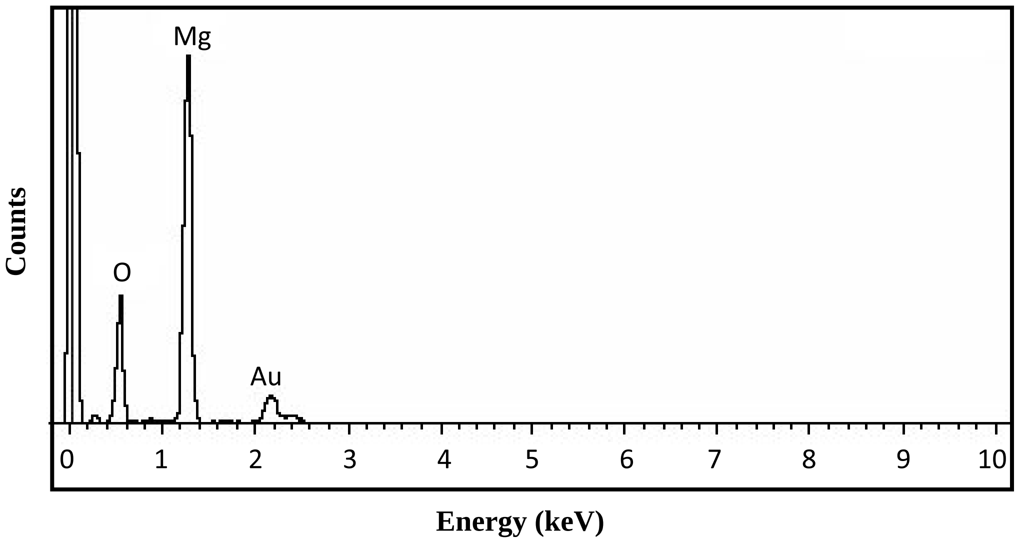

Fig. 4

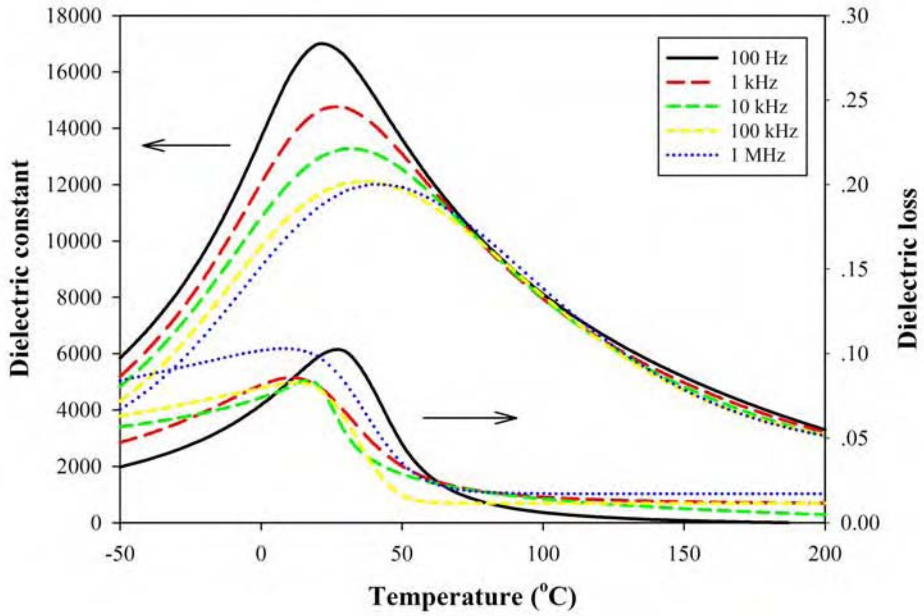
18000
16000
14000
12000
10000
8000
6000
4000
2000
0
Dielectric constant
.30
.25
.20
.15
.10
.05
0.00
Dielectric loss
-50
0
50
100
150
200
Temperature (^oC)
100 Hz
1 kHz
10 kHz
100 kHz
1 MHz

(a)

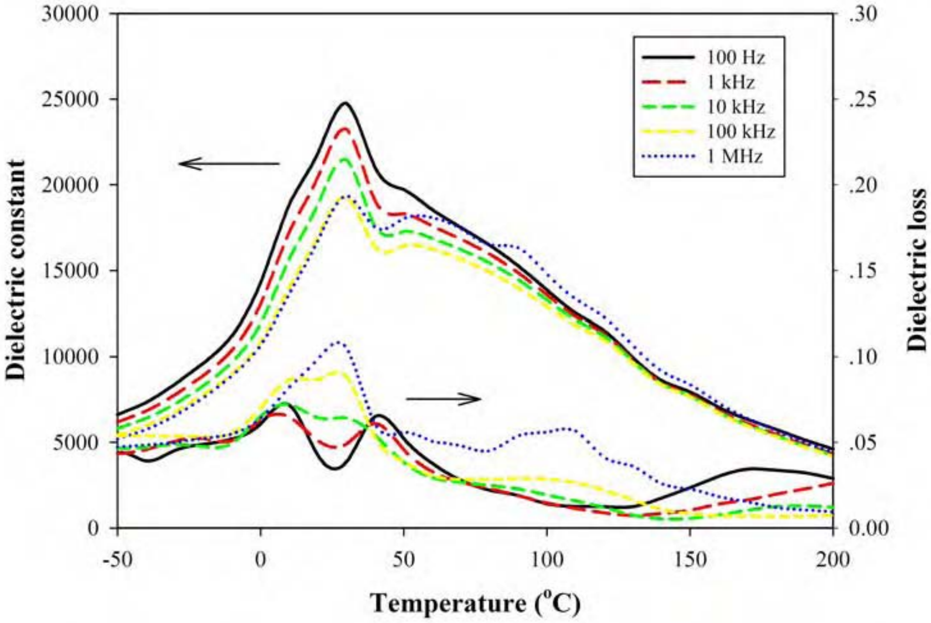
30000
25000
20000
15000
10000
5000
0
Dielectric constant
.30
.25
.20
.15
.10
.05
0.00
Dielectric loss
-50
0
50
100
150
200
Temperature (^oC)
100 Hz
1 kHz
10 kHz
100 kHz
1 MHz

(b)

Fig. 5

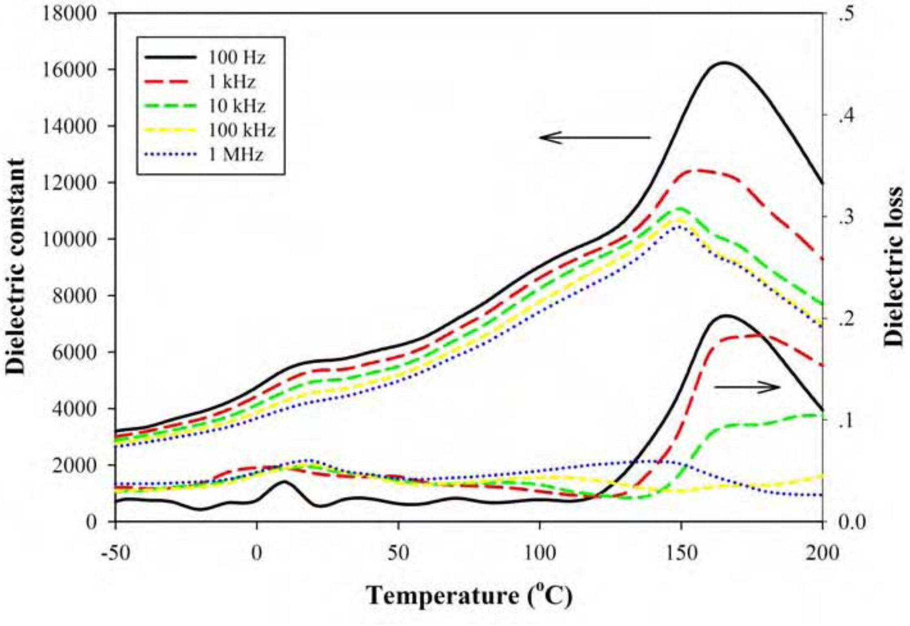
18000
16000
14000
12000
10000
8000
6000
4000
2000
0
.5
.4
.3
.2
.1
0.0
-50
0
50
100
150
200
100 Hz
1 kHz
10 kHz
100 kHz
1 MHz
Dielectric constant
Dielectric loss
Temperature (°C)

(a)

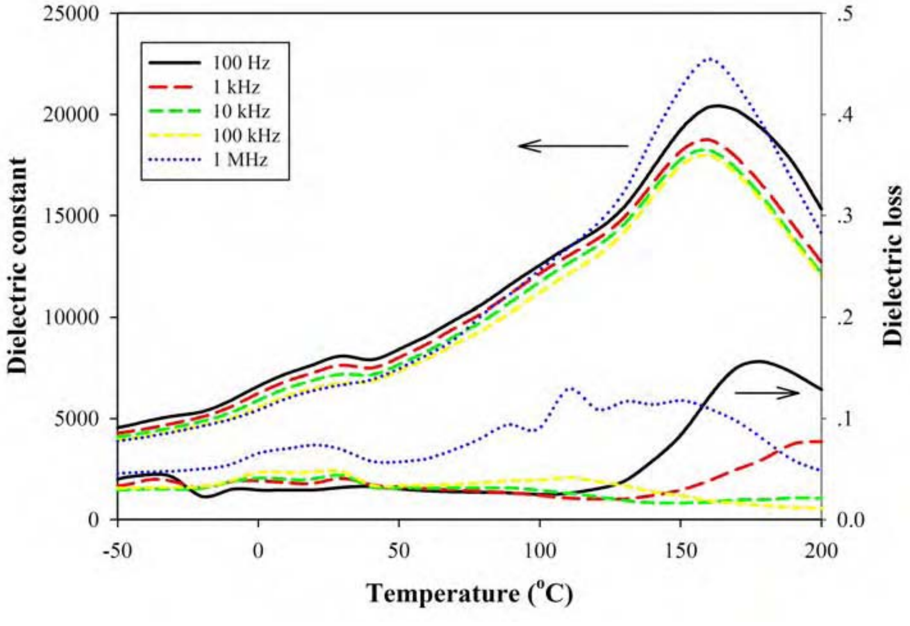
25000
20000
15000
10000
5000
0
.5
.4
.3
.2
.1
0.0
-50
0
50
100
150
200
100 Hz
1 kHz
10 kHz
100 kHz
1 MHz
Dielectric constant
Dielectric loss
Temperature (°C)

(b)

Fig. 6

3. การไปเสนอผลงานวิชาการ

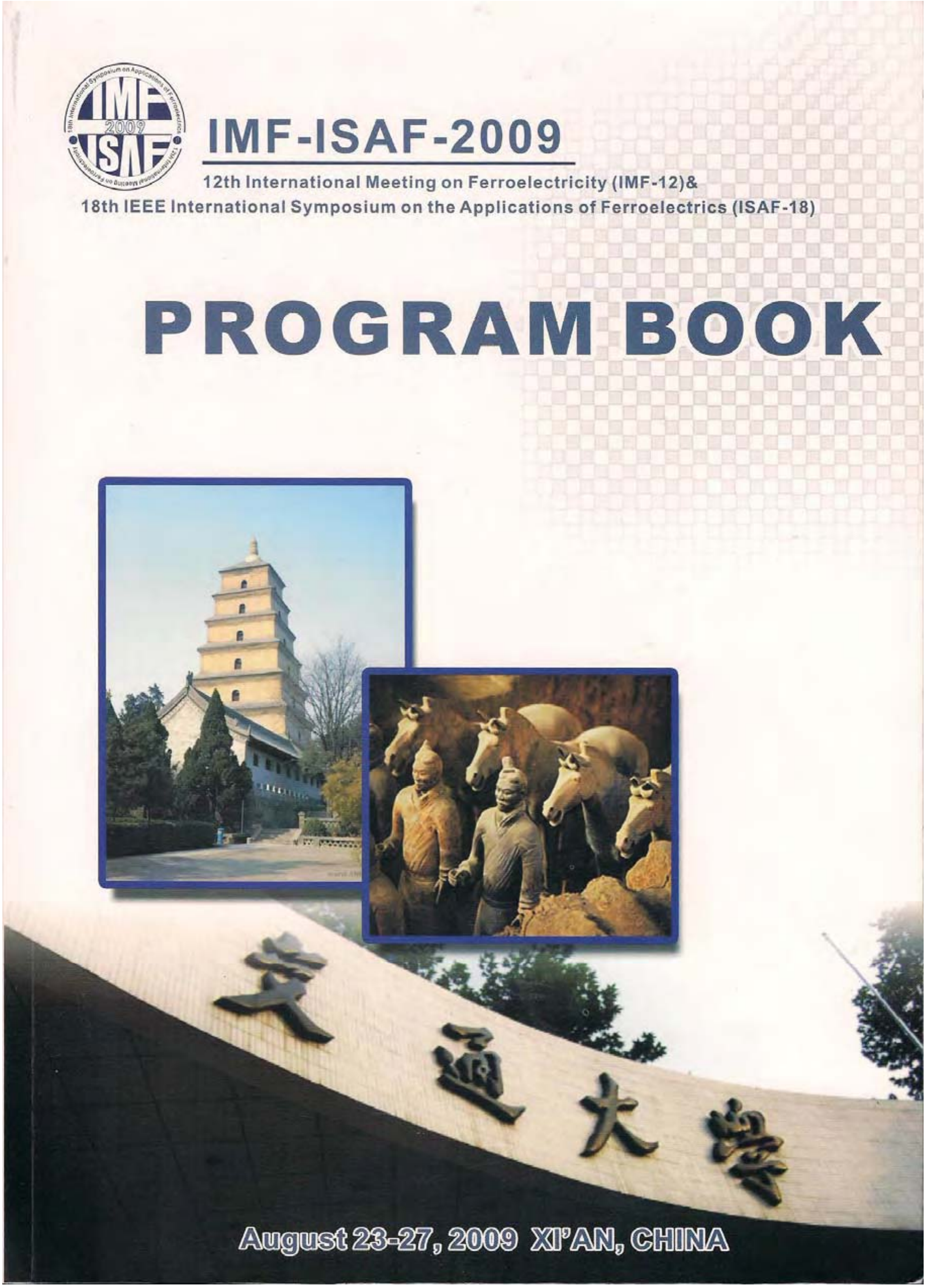

IMF-ISAF-2009

12th International Meeting on Ferroelectricity (IMF-12)&
18th IEEE International Symposium on the Applications of Ferroelectrics (ISAF-18)

PROGRAM BOOK

August 23-27, 2009 XI'AN, CHINA

IMF-IASF-2009
12TH INTERNATIONAL MEETING ON FERROELECTRICITY(IMF-12)&
18TH IEEE INTERNATIONAL SYMPOSIUM ON THE APPLICATIONS OF FERROELECTRICS(ISAF-18)
AUGUST 23-27, 2009 XI'AN, CHINA

April 12, 2009

Dr. Rewadee Wongmaneerung
Maejo University
Department of Physics, Faculty of Science, Maejo University
Thailand

Dear Dr. Rewadee Wongmaneerung:

We are pleased to inform you that your abstract entitled "**EFFECT OF ZINC OXIDE NANOWIRES ADDITION ON PHASE FORMATION, MICROSTRUCTURE AND DIELECTRIC PROPERTIES OF LEAD TITANATE CERAMICS**" by *R. Wongmaneerung, R. Yimnirun and S. Ananta* (Abstract ID: **CP-054.**) has been accepted for a poster presentation at IMF-ISAF-2009, which will be held in Shaanxi Zhangbagou Guesthouse, in Xi'an, China during August 23 to 27, 2009.

Registration and Visa Application for the IMF-ISAF-2009 conference are now available online at http://www.imf-isaf.com. Guideline for Registration and Visa Application are also posted on the conference website. Please register for the conference at your earliest convenience or before June 30th, 2009 to confirm your participation and to receive the lowest registration rates. At least one author is required to register for the conference for each accepted abstract in order for their papers to be included in the conference abstract book, and to be properly scheduled for presentation.

Please make hotel reservation at your earliest convenience for enjoying special rates. The Hotel Information is available at the conference website http://www.imf-isaf.com/hotels

The deadline for paper submission is *Midnight, August 24th, 2009, Beijing time*. The paper will be peer-reviewed. The author can submit his/her manuscript to be published in either a special issue of the journal "Ferroelectrics" published by Taylor & Francis or IEEE proceeding. The instruction for manuscript preparation has been posted on the conference website.

The complete program will be available online at http://www.imf-isaf.com/program.

We look forward to participation at IMF-ISAF-2009. See you in Xi'an, China.
Yours sincerely,

IMF-12 General Chair	ISAF-18 General Co-Chairs	
	W. Ren	Tadashi Takenaka
Prof. Yao Xi	Prof. Wei Ren	Prof. Tadashi Takenaka

EFFECT OF ZINC OXIDE NANOWIRES ADDITION ON PHASE FORMATION, MICROSTRUCTURE AND DIELECTRIC PROPERTIES OF LEAD TITANATE CERAMICS

R. Wongmaneerung[a], R. Yimnirun[b] and S. Ananta[b]
[a]Maejo University, Chiang Mai, Thailand 50290
[b]Chiang Mai University, Chiang Mai, Thailand 50200

Perovskite ferroelectric lead titanate ($PbTiO_3$ or PT) based ceramics which exhibit excellent dielectric, piezoelectric and pyroelectric properties have been widely employed in sensor, transducer and actuator applications, especially for devices working at high temperature and high frequency conditions [1-3]. However, pure and dense PT ceramic is regarded to be one of the most difficult lead-based perovskite ferroelectrics to produce especially via a simple solid-state reaction method [2,3]. To overcome such problems, a modified particle packing or composite techniques has been investigated. Recently, it was found that the presence of large amounts of semiconductor nanosized ZnO particles in the PZT matrix ceramics can result in a significantly increase of dielectric properties. Therefore, in this work, nanosized ZnO was chosen as semiconducting phase since it showed a negligible reaction with ferroelectric phase when the composites were sintered at high temperature.

Nanosized zinc oxide/lead titanate (ZnO/PT) ceramic matrix nanocomposites have been studied. Under an appropriate sintering condition, ZnO/PT ceramic nanocomposites were successfully fabricated by a pressureless sintering technique. Dependence of the dielectric properties of the ZnO/PT on frequency and temperature was determined. It has been found that a densification of the ceramic nanocomposites fabricated in this work was significantly enhanced, as compared to the conventional PT ceramics. Moreover, the high dielectric constant, which is higher than that of pure PT ceramics, was found in the ZnO/PT ceramic nanocomposites. The results showed that the addition of nanosized ZnO had an obvious influence on the dielectric properties of the ZnO/PT ceramic nanocomposites.

***Keywords*:** Lead titanate; zinc oxide; dielectric properties; nanocomposites

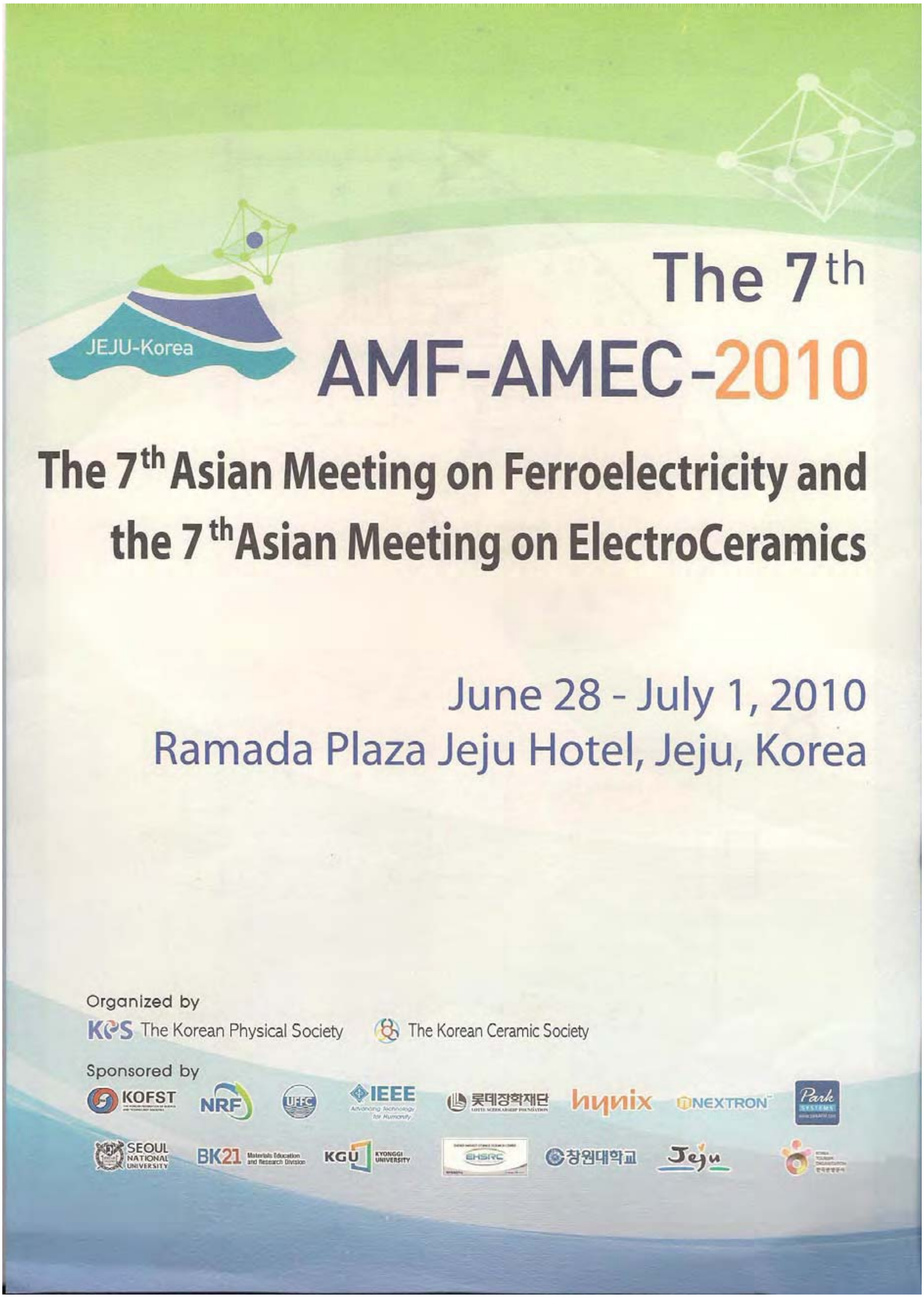

JEJU-Korea

The 7th AMF-AMEC-2010

The 7th Asian Meeting on Ferroelectricity and the 7th Asian Meeting on ElectroCeramics

June 28 - July 1, 2010
Ramada Plaza Jeju Hotel, Jeju, Korea

Organized by
KPS The Korean Physical Society
The Korean Ceramic Society

Sponsored by
KOFST NRF UFEC IEEE Advancing Technology for Humanity 롯데장학재단 hynix NEXTRON Park Systems
SEOUL NATIONAL UNIVERSITY BK21 Materials Education and Research Division KGU KYONGGI UNIVERSITY EHSRC 창원대학교 Jeju

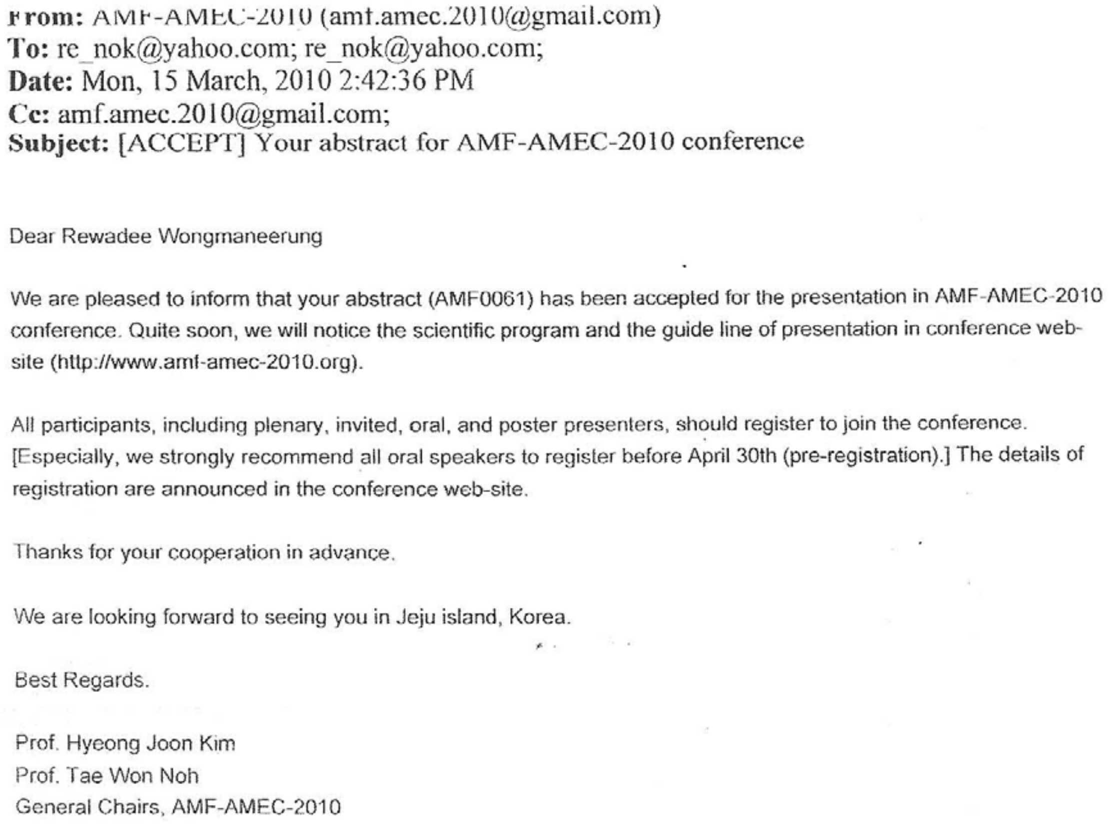

From: AMF-AMEC-2010 (amf.amec.2010@gmail.com)
To: re_nok@yahoo.com; re_nok@yahoo.com;
Date: Mon, 15 March, 2010 2:42:36 PM
Cc: amf.amec.2010@gmail.com;
Subject: [ACCEPT] Your abstract for AMF-AMEC-2010 conference

Dear Rewadee Wongmaneerung

We are pleased to inform that your abstract (AMF0061) has been accepted for the presentation in AMF-AMEC-2010 conference. Quite soon, we will notice the scientific program and the guide line of presentation in conference web-site (http://www.amf-amec-2010.org).

All participants, including plenary, invited, oral, and poster presenters, should register to join the conference. [Especially, we strongly recommend all oral speakers to register before April 30th (pre-registration).] The details of registration are announced in the conference web-site.

Thanks for your cooperation in advance.

We are looking forward to seeing you in Jeju island, Korea.

Best Regards.

Prof. Hyeong Joon Kim
Prof. Tae Won Noh
General Chairs, AMF-AMEC-2010

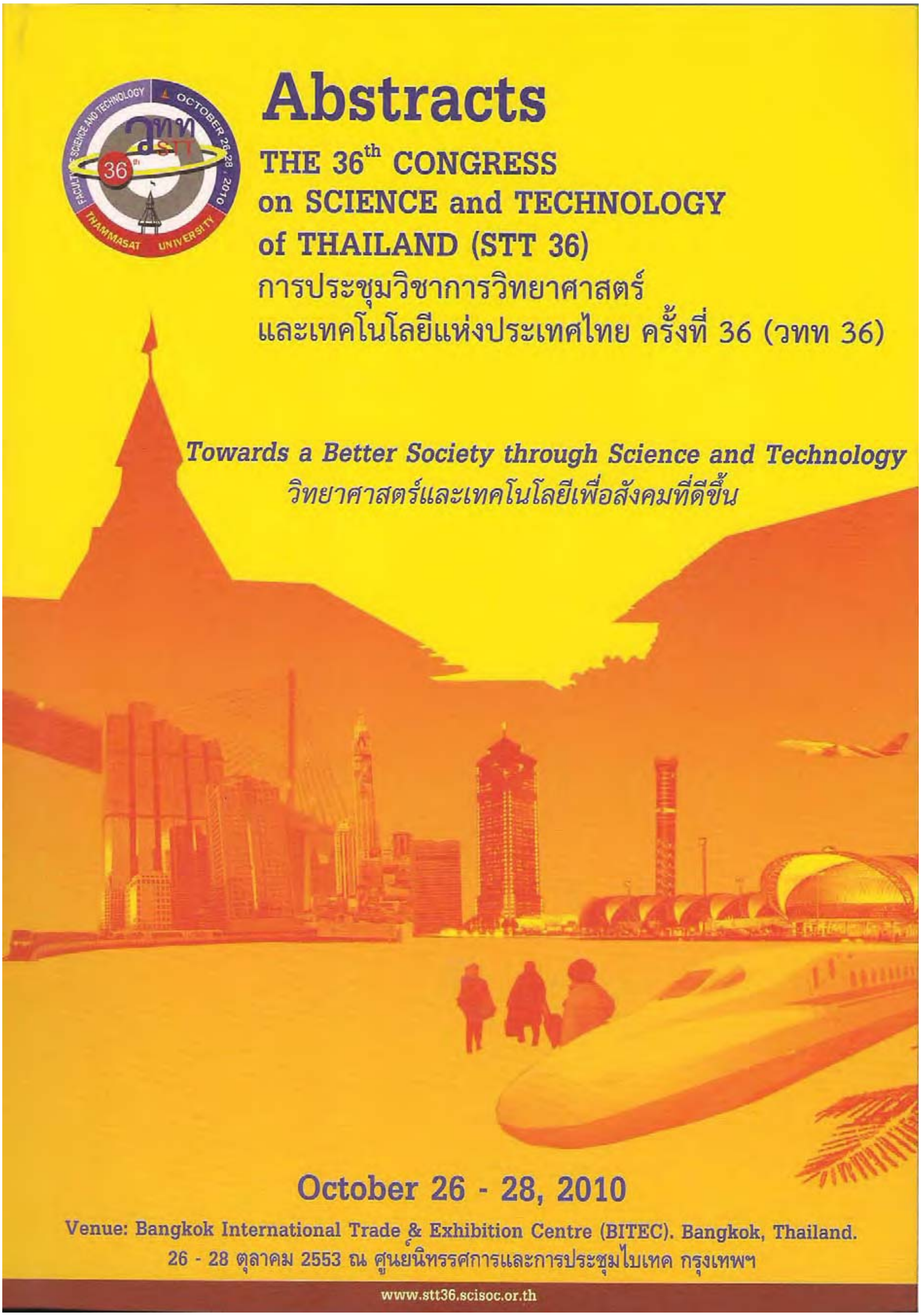

Abstracts

THE 36th CONGRESS
on SCIENCE and TECHNOLOGY
of THAILAND (STT 36)
การประชุมวิชาการวิทยาศาสตร์
และเทคโนโลยีแห่งประเทศไทย ครั้งที่ 36 (วทท 36)

Towards a Better Society through Science and Technology
วิทยาศาสตร์และเทคโนโลยีเพื่อสังคมที่ดีขึ้น

October 26 - 28, 2010

Venue: Bangkok International Trade & Exhibition Centre (BITEC). Bangkok, Thailand.
26 - 28 ตุลาคม 2553 ณ ศูนย์นิทรรศการและการประชุมไบเทค กรุงเทพฯ

www.stt36.scisoc.or.th

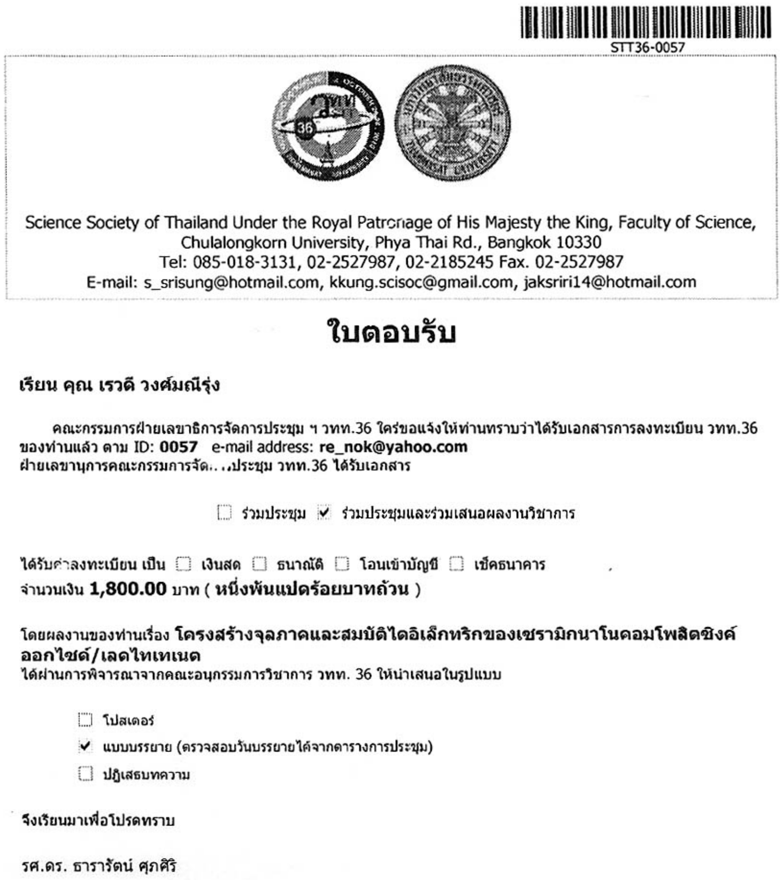

STT36-0057

Science Society of Thailand Under the Royal Patronage of His Majesty the King, Faculty of Science,
Chulalongkorn University, Phya Thai Rd., Bangkok 10330
Tel: 085-018-3131, 02-2527987, 02-2185245 Fax. 02-2527987
E-mail: s_srisung@hotmail.com, kkung.scisoc@gmail.com, jaksriri14@hotmail.com

ใบตอบรับ

เรียน คุณ เรวดี วงศ์มณีรุ่ง

คณะกรรมการฝ่ายเลขาธิการจัดการประชุม ฯ วทท.36 ใคร่ขอแจ้งให้ท่านทราบว่าได้รับเอกสารการลงทะเบียน วทท.36 ของท่านแล้ว ตาม ID: **0057** e-mail address: **re_nok@yahoo.com**
ฝ่ายเลขานุการคณะกรรมการจัด...ประชุม วทท.36 ได้รับเอกสาร

☐ ร่วมประชุม ☑ ร่วมประชุมและร่วมเสนอผลงานวิชาการ

ได้รับค่าลงทะเบียน เป็น ☐ เงินสด ☐ ธนาณัติ ☐ โอนเข้าบัญชี ☐ เช็คธนาคาร
จำนวนเงิน **1,800.00** บาท (**หนึ่งพันแปดร้อยบาทถ้วน**)

โดยผลงานของท่านเรื่อง **โครงสร้างจุลภาคและสมบัติไดอิเล็กทริกของเซรามิกนาโนคอมโพสิตซิงค์ออกไซด์/เลดไททาเนต**
ได้ผ่านการพิจารณาจากคณะอนุกรรมการวิชาการ วทท. 36 ให้นำเสนอในรูปแบบ

☐ โปสเตอร์
☑ แบบบรรยาย (ตรวจสอบวันบรรยายได้จากตารางการประชุม)
☐ ปฏิเสธบทความ

จึงเรียนมาเพื่อโปรดทราบ

รศ.ดร. ธารารัตน์ ศุภศิริ

โครงสร้างจุลภาคและสมบัติไดอิเล็กทริกของเซรามิกนาโนคอมโพสิตซิงค์ออกไซด์/เลดไทเทเนต

Microstructure and dielectric properties of ZnO/PT ceramic nanocomposites

เรวดี วงศ์มณีรุ่ง[1,*], รัตติกร ยิ้มนิรัญ[2], สุพล อนันตา[3]

Rewadee Wongmaneerung[1,*], Rattikorn Yimnirun[2], Supon Ananta[3]

[1] Department of Physics, Faculty of Science, Maejo University, Chiang Mai 50290, Thailand
[2] School of Physics, Institute of Science, Suranaree University of Technology,
Nakhon Ratchasima 30000, Thailand
[3] Department of Physics and Materials Science, Faculty of Science, Chiang Mai University,
Chiang Mai 50200, Thailand
*e-mail: re_nok@yahoo.com

บทคัดย่อ: ในงานวิจัยนี้ได้ศึกษาเกี่ยวกับโครงสร้างจุลภาคและสมบัติไดอิเล็กทริกของเซรามิกนาโนคอมโพสิตซิงค์ออกไซด์/เลดไทเทเนต โดยเริ่มต้นจากการประดิษฐ์เซรามิกนาโนคอมโพสิตซิงค์ออกไซด์/เลดไทเทเนต ซึ่งใช้ซิงค์ออกไซด์ในอัตราส่วนที่แตกต่างกัน นำเซรามิกที่ผ่านการขึ้นรูปมาเผาซินเตอร์ภายใต้เงื่อนไขต่างๆ จากนั้นทดสอบการเกิดเฟส โครงสร้างจุลภาค และสมบัติไดอิเล็กทริกด้วยเครื่องเอ็กซเรย์ดิฟแฟรคชัน สแกนนิ่งอิเล็กตรอนไมโครสโคป และเครื่องแอล ซี แซดมิเตอร์ ตามลำดับ ผลการทดลองพบว่าเมื่อเผาซินเตอร์ภายใต้เงื่อนไขที่เหมาะสมสามารถประดิษฐ์เซรามิกนาโนคอมโพสิตที่มีความบริสุทธิ์และความหนาแน่นสูงได้ นอกจากนี้ยังมีค่าคงที่ไดอิเล็กทริกที่สูงกว่าเมื่อเปรียบเทียบกับเซรามิกเลดไทเทเนต

Abstract: Ceramic nanocomposites of zinc oxide (ZnO) nanowhiskers in lead titanate ($PbTiO_3$ or PT) matrix were successfully fabricated by a pressureless sintering technique. Phase formation, densification, microstructure and dielectric properties of the composites were investigated as a function of ZnO content. It has been found that a densification of the ceramic nanocomposites fabricated in this work was significantly enhanced, as compared to the conventional PT ceramics. Moreover, the high dielectric constant, which is higher than that of the monolithic PT ceramics, was found in the PT/ZnO ceramic nanocomposites.

Introduction: Dense perovskite lead titanate ($PbTiO_3$ or PT) based ceramics which exhibit many of the desirable dielectric, piezoelectric and pyroelectric properties for use in electronic and electro-optic devices at high temperature and high frequency [1-2]. However, it is well known today that PT ceramics, if at all pure and dense, break up into a powder when they are cooled through the Curie point due to large distortion of the tetragonal phase at room temperature which is characterized by the ratio between the lattice parameter (c/a, ~1.06 [3]). To overcome such problems, several techniques have been introduced. One approach is to try to modify it with small amounts of additives [4] but the results do not necessarily illuminate the properties of the pure substance, which is of interest in its own right. Furthermore, utilizing nanopowders, employing spark-plasma sintering and carrying out appropriated

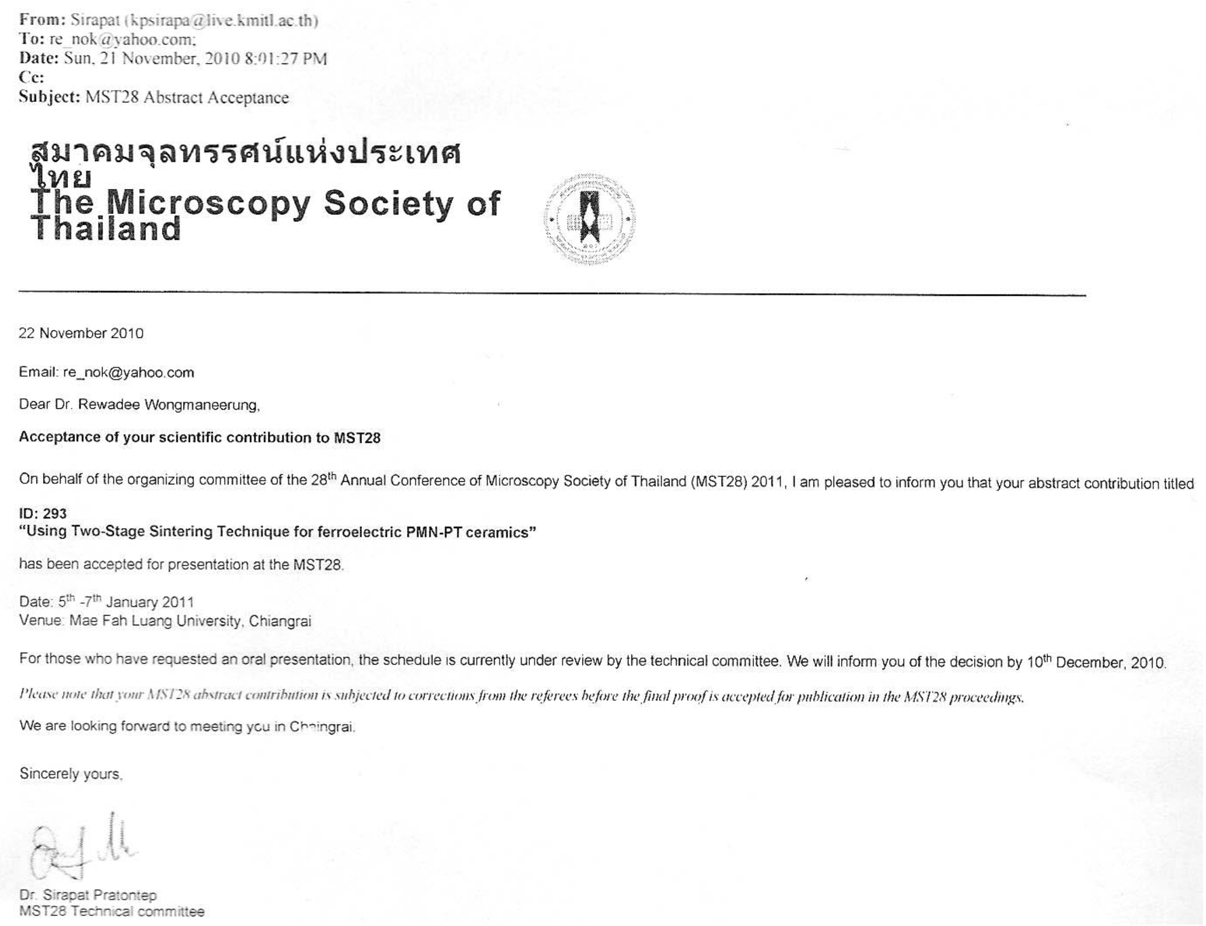

From: Sirapat (kpsirapa@live.kmitl.ac.th)
To: re_nok@yahoo.com;
Date: Sun, 21 November, 2010 8:01:27 PM
Cc:
Subject: MST28 Abstract Acceptance

สมาคมจุลทรรศน์แห่งประเทศไทย
The Microscopy Society of Thailand

---

22 November 2010

Email: re_nok@yahoo.com

Dear Dr. Rewadee Wongmaneerung,

Acceptance of your scientific contribution to MST28

On behalf of the organizing committee of the 28th Annual Conference of Microscopy Society of Thailand (MST28) 2011, I am pleased to inform you that your abstract contribution titled

ID: 293
"Using Two-Stage Sintering Technique for ferroelectric PMN-PT ceramics"

has been accepted for presentation at the MST28.

Date: 5th -7th January 2011
Venue: Mae Fah Luang University, Chiangrai

For those who have requested an oral presentation, the schedule is currently under review by the technical committee. We will inform you of the decision by 10th December, 2010.

Please note that your MST28 abstract contribution is subjected to corrections from the referees before the final proof is accepted for publication in the MST28 proceedings.

We are looking forward to meeting you in Chaingrai.

Sincerely yours,

Dr. Sirapat Pratontep
MST28 Technical committee

er Presentation

Two-Stage Sintering Technique for Ferroelectric PMN-PT Ceramic Fabrication

ngmaneerung [1*], R. Yimnirun [2], S. Ananta [3]
rials Science Program, Faculty of Science, Maejo University, Chiang Mai, Thailand
l of Physics, Institute of Science, Suranaree University of Technology, Nakhon Ratchasima, Thailand,
rtment of Physics and Materials Science, Faculty of Science, Chiang Mai University, Chiang Mai,
land
responding author, e-mail: re_nok@yahoo.com

---

tract

Sintering is a complicated process of microstructure evolution, with the main outcome being porosity ation [1-3]. This process is a thermal treatment for bonding particles into a coherent, predominantly solid ure via mass transport. The bonding leads to improved strength and a lower system energy [4]. The onset accelerated grain growth depends on the microstructure; a uniform size and shape distribution of pores and s postpones accelerated grain growth [5]. Such collapse results in a substantial decrease in pore pinning, triggers accelerated grain growth [6,7]. The prevailing sintering paradigm is to mitigate this undesirable ome by suppressing grain boundary mobility. The aim is to maintain pore-grain boundary contact during n growth so that pore breakaway never occurs.

Lead magnesium niobate-lead titanate ((1-x)PMN–xPT) has attracted a growing fundamental and practical est because of their excellent dielectric, piezoelectric and electrostriction properties which are useful in ronic devices. For high performance it is essential that the material be of the perovskite crystalline phase n no pyrochlore phase. In the processing of perovskite PMN–PT, the formation of an unwanted pyrochlore e and high density has long been recognized as a major problem. In our previous work, a two-stage ring technique has been succeed to achieve the purification and densification of PMN ceramic. However, so far, no work has been done on the investigation of the two-stage sintering PMN-PT ceramics.

Therefore, in this study, effects of two-stage sintering on phase formation, microstructure and dielectric properties of PMN-PT ceramics were investigated via XRD, SEM and dielectric measurement. Pure and dense perovskite ceramics of PMN-PT have been successfully fabricated by using a two-stage sintering technique. In general, the grains are similar in shape. Micrograph shows a few pores at triple points. In addition, it is seen that the PMN-PT samples also have an intergranular fracture mechanism, indicating that the grain boundaries are mechanically weaker than the grains. Moreover, this work demonstrated that under suitable two-stage sintering schemes, dense and pure perovskite PMN-PT ceramics can be successfully achieved with better dielectric properties than those of ceramics from a conventional methods.

References

1. R.L. Coble, J.E. Burke, Sintering in Ceramics, in Progress in Ceramic Science, Vol. 3, Edited by J. E. Burke, Pergamon Press, New York, 1963, pp. 197-251.
2. R.J. Brook, Controlled Grain Growth, in Treatise on Materials Science and Technology, Vol. 9, Edited by F. F. Y. Wang, Academic Press, New York, 1976, pp. 331-64.
3. R.L. Coble, R.M. Cannon, Current Paradigms in Powder Processing, Mater. Sci. Res, 11, 151 (1978).
4. R.M. German, Sintering Theory and Practice, John Wiley & Son, New York, 1996, pp.8-9.
5. C.P. Cameron, R. Raj, Grain Growth Transition During Sintering of Colloidally Prepared Alumina Powder Compacts, J. Am. Ceram. Soc., 71 [12], 1031-5 (1988).
6. R.L. Coble, Sintering Crystalline Solids. I. Intermediate and Final State Diffusion Models, J. Appl. Phys., 32 [5], 787-92 (1961).
7. R.L. Coble, Sintering Crystalline Solids. II. Experimental Test of Diffusion Models in Powder Compacts, J. Appl. Phys., 32 [5], 793-9 (1961).

4. รางวัลที่ได้รับ

แม่โจ้ 2552-2553

ปีแห่งคุณภาพและเกียรติประวัติ

MAEJO 2009-2010 : the year of quality and glory

มหาวิทยาลัยแม่โจ้

ขอมอบเกียรติบัตรนี้ไว้เพื่อแสดงว่า

อาจารย์ ดร.เรวดี วงศ์มณีรุ่ง

ได้รับรางวัล

นักวิจัยรุ่นใหม่ สาขาวิทยาศาสตร์และเทคโนโลยี

ให้ไว้ ณ วันที่ ๒ กรกฎาคม พุทธศักราช ๒๕๕๓

ขอให้ท่านประสบความเจริญก้าวหน้าในหน้าที่การงานตลอดไป

(รองศาสตราจารย์ ดร.เทพ พงษ์พานิช)
อธิการบดีมหาวิทยาลัยแม่โจ้

คณะวิทยาศาสตร์ มหาวิทยาลัยแม่โจ้
ขอมอบเกียรติบัตรฉบับนี้ให้ไว้ เพื่อแสดงว่า

อาจารย์ ดร.เรวดี วงศ์มณีรุ่ง

ได้รับรางวัลผลงานวิจัยที่ได้รับการอ้างอิงสูงสุด ประจำปีงบประมาณ ๒๕๕๒

ขอจงมีความเจริญด้วยจตุรพิธพร ทำคุณประโยชน์ในด้านการสร้างสรรค์ปัญญา
เพื่อพัฒนาประเทศสืบต่อไปชั่วกาลนาน

(ผู้ช่วยศาสตราจารย์พึ่งพร เนียมทรัพย์)
คณบดีคณะวิทยาศาสตร์